This work has been submitted to the IEEE for possible publication.

© 2025 IEEE. Personal use of this material is permitted. Permission from IEEE must be obtained for all other uses, in any current or future media, including reprinting/republishing this material for advertising or promotional purposes, creating new collective works, for resale or redistribution to servers or lists, or reuse of any copyrighted component of this work in other works.

Copyright may be transferred without notice, after which this version may no longer be accessible.

Differential Space-Time Block Coding for Phase-Unsynchronized Cell-Free MIMO Downlink

Marx M. M. Freitas, *Member, IEEE*, Giovanni Interdonato, *Member, IEEE*, and Stefano Buzzi, *Senior Member, IEEE*

Abstract-In the downlink of a cell-free massive multipleinput multiple-output (CF-mMIMO) system, spectral efficiency gains critically rely on joint coherent transmission, as all access points (APs) must align their transmitted signals in phase at the user equipment (UE). Achieving such phase alignment is technically challenging, as it requires tight synchronization among geographically distributed APs. In this paper, we address this issue by introducing a differential space-time block coding (DSTBC) approach that bypasses the need for AP phase synchronization. We first provide analytic bounds to the achievable spectral efficiency of CF-mMIMO with phase-unsynchronized APs. Then, we propose a DSTBC-based transmission scheme specifically tailored to CF-mMIMO, which operates without channel state information and does not require any form of phase synchronization among the APs. We derive a closedform expression for the resulting signal-to-interference-plus-noise ratio (SINR), enabling quantitative comparisons among different DSTBC schemes. Numerical simulations confirm that phase misalignments can significantly impair system performance. In contrast, the proposed DSTBC scheme successfully mitigates these effects, achieving performance comparable to that of fully synchronized systems.

Index Terms—Cell-free Massive MIMO, phase misalignment, differential space-time block-coding.

I. INTRODUCTION

User-centric (UC) cell-free massive multiple-input multiple-output (CF-mMIMO) systems stand as a pivotal architecture for enabling next-generation wireless networks, including 6G and beyond [3], [4]. Moving beyond traditional cellular structures, CF-mMIMO employs a large ensemble of geographically distributed APs that collaboratively serve multiple UEs. This distributed coordination approach yields several substantial advantages over conventional deployments. Foremost among these benefits is the provision of a significantly more spectral efficiency (SE) across the entire service area, effectively mitigating performance bottlenecks often experienced by UEs situated at cell boundaries. Furthermore, the inherent redundancy provided by the numerous distributed connection

This work was supported by the EU under the Italian National Recovery and Resilience Plan (NRRP) of NextGenerationEU, partnership on "Telecommunications of the Future" (PE00000001 - program "RESTART"); specifically, Structural Project NTN, Cascade Call INFINITE, CUP D93C22000910001, and Structural Project 6GWINET, Cascade Call SPARKS, CUP D43C22003080001. A preliminary and shortened version of the technical content presented here is reported in [1], whereas [2] limits its analysis to unmanned aerial vehicle-empowered aerial cell-free massive MIMO systems adopting a differential Alamouti code scheme.

The authors are with the Dept. of Electrical and Information Engineering (DIEI), University of Cassino and Southern Lazio, 03043 Cassino, Italy (e-mail:{marxmiguelmiranda.defreitas; buzzi; giovanni.interdonato}@unicas.it). S. Buzzi and G. Interdonato are also with the Consorzio Nazionale Interuniversitario per le Telecomunicazioni (CNIT), 43124 Parma, Italy. S. Buzzi is also with the Dipartimento di Elettronica, Informazione e Bioingegneria (DEIB), Politecnico di Milano, 20156 Milan, Italy.

paths substantially enhances system resilience against effects such as link blockages and deep shadow fading, offering crucial support for high-mobility users and ultra-reliable low-latency communication (URLLC) [5]. Achieving scalability and energy efficiency through techniques like local processing and UC clustering further underscores the attractiveness of CF-mMIMO as a foundational technology.

In order to fully realize the performance potential afforded by the network-wide coordination of APs, the downlink (DL) transmission critically requires joint coherent transmission. This necessity mandates that the signals transmitted from all serving APs arrive at the targeted UE antenna perfectly aligned in phase, ensuring maximal constructive combination. However, maintaining such stringent phase synchronization is highly demanding in practical implementations. Each AP operates using its own local, independent oscillator to modulate the data-carrying signal, resulting in distinct and uncontrollable phase offsets across the network. These uncompensated phase misalignments directly violate the assumption of coherent transmission, leading to phase distortions in the effective DL channel vector. As a result, the desired signals may combine destructively, causing severe degradation in the received signal power and significantly impairing the achievable DL SE.

A. Related Works and Motivation

Mitigating AP phase misalignments in CF-mMIMO systems remains a significant challenge. Most current literature focuses on mitigating the effects of these misalignments rather than developing inherently immune transmission schemes.

One major research thrust involves over-the-air (OTA) synchronization and time-division duplex (TDD) reciprocity calibration protocols [6]–[13]. While pioneering, these methods often suffer from high computational complexity at the central processing unit (CPU) [6] or introduce significant measurement overhead that can degrade spectral efficiency (SE) as the number of APs increases [13].

Another set of works first analyzed the severe performance degradation caused by asynchronous reception and oscillator phase noise (PN) [14]–[16]. Subsequent proposals for robust precoding schemes [17]–[19] attempt to counter these effects. However, these solutions often rely on impractical assumptions like perfect channel state information (CSI) [17], are only effective in extreme mismatch scenarios [18], or lose their performance gains under severe phase uncertainties [19].

Recognizing the difficulty of achieving full coherence, a third approach relaxes synchronization requirements. This includes hybrid AP grouping [20], partially coherent (PC) transmission [21], [22], and non-coherent (NC) joint transmission [23], [24]. While these schemes can be effective under

certain constraints, they introduce new challenges, such as feedback overhead for UE-assisted grouping [20], performance reliance on cluster tuning [21], or fundamental signal-to-noise ratio (SNR) and capacity losses compared to the ideal coherent case [24], [25].

These strategies all fail to fully mitigate phase misalignments. Residual errors persist, and many methods depend on high-quality CSI, which is unreliable under pilot contamination. Motivated by this gap, our previous works [1], [2] proposed DSTBC techniques [26] as an alternative that inherently removes the need for AP phase synchronization. While this approach successfully restored SE and bit-error rate (BER) performance, the analysis had practical limitations. Specifically, the maximum likelihood (ML) detector used in [1], [2] incurred high computational complexity, and the analytical proof of phase cancellation relied on an idealistic assumption of perfect signal detection.

B. Main Contributions

This paper extends our studies [1], [2] by developing a comprehensive analytical framework for DSTBC-based CF-mMIMO that overcomes the limitations identified in Section I-A. We provide a quantitative assessment of DSTBC performance, demonstrating its potential to achieve synchronous-like performance in asynchronous environments. The main contributions are:

- We develop a DSTBC methodology based on *amicable orthogonal designs*, $\{\mathbf{A}_n\}_{n=1}^{n_s}$ and $\{\mathbf{B}_n\}_{n=1}^{n_s}$, that mitigates phase misalignments. We show that this structure decouples the ML detection criterion into n_s per-symbol terms. This enables low-complexity, individual symbol detection, overcoming the high-complexity ML detection limitation of [1], [2] and representing a novel approach for CF-mMIMO.
- We rigorously prove the phase mitigation capability of DSTBC without the ideal assumption of perfect detection used in [1]. Our derivation shows the desired signal component depends only on the magnitude squared of the effective DL channel, confirming the cancellation of phase misalignment terms under realistic conditions.
- We derive novel analytical expressions for the DL SINR of conventional CF-mMIMO under phase misalignments.
 These expressions, new to the literature, explicitly characterize the SINR decay as a function of the average phase misalignment at the APs.
- Based on these SINR results, we derive closed-form achievable SE expressions for conventional systems using maximum ratio (MR) precoding, enabling direct performance evaluation without extensive simulations.
- For the proposed DSTBC scheme, we derive an approximate SNR expression for the single-user scenario to provide a baseline understanding of its resilience.
- We derive a comprehensive, approximate SINR expression for the general multi-user DSTBC CF-mMIMO system. This expression accounts for residual noise and multi-user interference from the differential detection process, with closed-form calculations for signal and in-

terference components. It enables performance evaluation without relying on intensive Monte Carlo simulations.

C. Organization and Notation

The paper is organized as follows: Section I provides the necessary background and motivation, while Section II details the system model. The core contributions, which involve the DSTBC approach designed to mitigate phase misalignment effects, are presented in Section III. In Section IV, we present the numerical results demonstrating the effectiveness of our proposed approach. Lastly, Section V summarizes the findings and conclusions of this study.

Notation: Boldface lowercase and uppercase letters denote vectors and matrices, respectively. The superscripts $(\cdot)^T$ and $(\cdot)^H$ denote the transpose and the conjugate-transpose operations, respectively. The $N\times N$ identity matrix is denoted as \mathbf{I}_N , and the cardinality of the set \mathcal{A} is represented by $|\mathcal{A}|$. The trace and euclidean norm are denoted as $\operatorname{tr}(\cdot)$ and $\|\cdot\|$, and $[\cdot]$ is the floor operation. $\mathcal{N}_{\mathbb{C}}(\mu,\sigma^2)$ stands for a complex Gaussian random variable with mean μ and variance σ^2 . $\mathbf{A} = \operatorname{diag}(\mathbf{a})$ yields a diagonal matrix with the elements of the vector \mathbf{a} on the diagonal, and $\mathbf{a} = \operatorname{diag}(\mathbf{A})$ yields a vector given by the diagonal elements of \mathbf{A} . The operator $\angle \cdot$ denotes the phase.

II. SYSTEM MODEL

We consider a CF-mMIMO system consisting of K singleantenna UEs and L APs, each equipped with N antennas, geographically distributed into the coverage area. The APs connect to a CPU via fronthaul links, which are assumed to be error-free and able to support the data traffic [3]. The system operates on TDD mode and assumes that the uplink (UL) and DL channels are reciprocal. Hence, channel estimation is performed only in the UL direction. The channel $\mathbf{h}_{k,l} \in \mathbb{C}^N$ between the UE k and AP l undergoes an independent correlated Rayleigh fading realization, being defined as $\mathbf{h}_{k,l} \sim \mathcal{N}_{\mathbb{C}}(\mathbf{0}, \mathbf{R}_{k,l})$, where $\mathbf{R}_{k,l} = \mathbb{E}_{\mathbf{h}}\{\mathbf{h}_{k,l}\mathbf{h}_{k,l}^{\mathrm{H}}\} \in \mathbb{C}^{N \times N}$ is the statistical covariance matrix of the channel. The operator \mathbb{E}_{h} indicates that the expectations are taken with respect to the channel realizations. The channels of different APs are assumed to be uncorrelated, i.e., $\mathbb{E}_{\mathbf{h}}\{\mathbf{h}_{k,l}\mathbf{h}_{k,l'}^{\mathrm{H}}\}=\mathbf{0}$, $\forall l \neq l'$, as the APs are placed several wavelengths apart to ensure macrodiversity. The covariance matrices are assumed to remain constant over multiple coherence blocks, while the channels $\{\mathbf{h}_{k,l}\}$ vary independently from block to block.

A. Phase Misalignment and UL Training

The impact of phase misalignment in the DL channels of CF-mMIMO systems is commonly modeled by introducing an uncompensated phase component into the channel vector between UE k and AP l. As a result, the true channel between the UE k and AP l is given by $\mathbf{g}_{k,l} = e^{-j\vartheta_l}\mathbf{h}_{k,l}$, where ϑ_l represents the oscillator phase in the transmit chain of AP l. This phase may also include phase noise effects, and is assumed to stay constant for at least the time needed to send

¹The statistical covariance matrix captures the large-scale fading effects, namely the spatial channel correlation, path loss, and shadowing [3].

two consecutive DSTBC codewords, i.e., for a few symbol intervals [26]. We model the oscillator phases ϑ_l as uniformly distributed random variables over the interval $[-\alpha, \alpha]$, i.e., $\vartheta_l \sim \mathcal{U}[-\alpha, \alpha]$ for $l = \{1, ..., L\}$.

As we focus on DL channels, let us consider that each coherence block contains τ_c samples, with τ_d samples being reserved for DL data and τ_p for UL pilot signals. During the UL training phase, the UEs send pilot sequences of τ_p -length to the APs for channel estimation. The pilot signals are assumed to be mutually orthogonal and independent of the number of UEs K to ensure the scalability of the pilot resources. Let $\mathcal{Q}_k \subset \{1,\ldots,K\}$ denote the subset of the UEs assigned to the pilot q_k , including the UE k. The received pilot signal at AP l can be expressed as [3]

$$\mathbf{y}_{q_k,l}^{\text{pilot}} = \sum\nolimits_{i \in \mathcal{Q}_k} \sqrt{\tau_p \eta_i} \, e^{-j\vartheta_l} \mathbf{h}_{i,l} + \mathbf{n}_{q_k,l}, \tag{1}$$

where η_i is the power with which UE i transmits the pilot symbol and $\mathbf{n}_{q_k,l} \sim \mathcal{N}_{\mathbb{C}}\left(\mathbf{0}_N, \sigma_{\mathrm{ul}}^2 \mathbf{I}_N\right)$ is additive noise at the receiver. Assuming that the covariance matrix $\mathbf{R}_{k,l}$ is perfectly known at the APs and CPU, the minimum mean square error (MMSE) estimate of the channel $\mathbf{h}_{k,l}$ is given by [3]

$$\widehat{\mathbf{h}}_{k,l} = \sqrt{\tau_p \eta_k} \mathbf{R}_{k,l} \mathbf{\Psi}_{q_k,l}^{-1} \mathbf{y}_{q_k,l}^{\text{pilot}},$$
 (2)

where $\Psi_{q_k,l} = \mathbb{E}_{\mathbf{h}}\{(\mathbf{y}_{q_k,l}^{\mathrm{pilot}})(\mathbf{y}_{q_k,l}^{\mathrm{pilot}})^{\mathrm{H}}\}$ represents the covariance matrix of the received pilot signal $\mathbf{y}_{q_k,l}^{\mathrm{pilot}}$, being calculated as

$$\Psi_{q_k,l} = \sum_{i \in \mathcal{Q}_k} \eta_i \tau_p \mathbf{R}_{i,l} + \sigma_{\text{ul}}^2 \mathbf{I}_N.$$
 (3)

B. AP Clustering and DL Data Transmission

In UC CF-mMIMO systems, each UE is served by a subset of APs. The association between the generic k-th UE and the APs can be modeled with the vector $\mathbf{a}_k \in \mathbb{C}^{L \times 1}$, in which the element $\mathbf{a}_{k,l}$ is 1 if AP l provides service to UE k, implying that $l \in \mathcal{M}_k$, and $\mathbf{a}_{k,l}$ is 0 otherwise. Here, $\mathcal{M}_k \subset \{1,\ldots,L\}$ denotes the subset of APs serving the UE k. Moreover, each AP is assumed to serve a limited number of UEs, denoted by K_{\max} , to prevent its computational load from scaling with the number of UEs K in the network, with $K_{\max} \leq \tau_p$ [3], [27]. Therefore, by letting \mathcal{K}_l denote the subset of UEs served by AP l, one can note that $|\mathcal{K}_l| \leq K_{\max}$.

Once the UE's AP cluster is defined, the precoding vector $\mathbf{w}_{k,l} \in \mathbb{C}^{N \times 1}$ between the UE k and the AP l is generated, for all APs in \mathcal{M}_k . The precoding vectors can be computed locally at each AP or centrally at the CPU. The precoding vector $\mathbf{w}_{k,l}$ also satisfies $\mathbb{E}_{\widehat{\mathbf{h}}} \big\{ \left\| \mathbf{w}_{k,l} \right\|^2 \big\} = \rho_{k,l}$, where $\rho_{k,l} \leq \rho_{\max}$ is the fraction of power allocated to the UE k regarding the AP l. Here, ρ_{\max} represents the maximum transmit power at each AP. After generating the precoding vectors, all APs in \mathcal{M}_k jointly transmit the same data symbol to UE k in DL coherent transmissions. Let $\sum_{i=1}^K \mathbf{a}_{i,l}\mathbf{w}_{i,l}s_i^p \in \mathbb{C}^{N \times 1}$ denote the data signal transmitted by AP l at discrete time epoch $p = \{1, \dots, \tau_d\}$, where s_i^p is the complex symbol intended for UE k. Moreover, let us denote

$$\mathbf{g}_{k,l}^{(\text{ef})} = \mathbf{a}_{k,l} \mathbf{g}_{k,l}^{\mathbf{H}} \mathbf{w}_{k,l} = \mathbf{a}_{k,l} e^{j\vartheta_l} \mathbf{h}_{k,l}^{\mathbf{H}} \mathbf{w}_{k,l}, \qquad (4)$$

$$\widetilde{\mathbf{g}}_{i,k,l}^{(\text{ef})} = \mathbf{a}_{i,l} \, e^{j\vartheta_l} \mathbf{h}_{k,l}^{\mathrm{H}} \mathbf{w}_{i,l} \,, \tag{5}$$

as the *effective* DL channels of the UE k, and the interfering UE i, respectively, with respect to AP l, for $k \neq i$. As a result,

the received signal at UE k can be expressed as

$$y_k^p = \sum_{l=1}^L g_{k,l}^{(\text{ef})} s_k^p + \sum_{l=1}^L \sum_{i=1, i \neq k}^K \widetilde{g}_{i,k,l}^{(\text{ef})} s_i^p + n_k^p, \tag{6}$$

where $n_k^p \sim \mathcal{N}_{\mathbb{C}}(0,\sigma_{\mathrm{dl}}^2)$ is the receiver noise. Assuming that the phase-shift keying (PSK) modulation² is used, the detection of s_k^p given y_k^p can be performed using the ML criterion $\hat{s}_k^p = \arg\min_{s \in \mathcal{S}} \left| \angle y_k^p - \angle s \right|^2$.

C. Precoding and Power Allocation Schemes

UC CF-mMIMO systems are implemented using either centralized or distributed processing. In distributed processing, channel estimation and precoding design are performed locally in the APs. In contrast, in centralized processing, these tasks are performed in the CPU. The centralized processing typically achieves higher SE and requires less signaling on the fronthaul links, as the CPU has access to the global CSI. In contrast, the distributed processing demands less computational complexity.

To compute the precoding vectors in a scalable way, the UL/DL duality is considered. In distributed processing, $\mathbf{w}_{k,l}$ is selected based on its local channel estimates as

$$\mathbf{w}_{k,l} = \sqrt{\rho_{k,l}} \frac{\overline{\mathbf{w}}_{k,l}}{\sqrt{\mathbb{E}_{\widehat{\mathbf{h}}}\{\|\overline{\mathbf{w}}_{k,l}\|^2\}}},$$
 (7)

where $\overline{\mathbf{w}}_{k,l}$ defines the direction of the precoding vector. In centralized processing, the collective precoding vector $\mathbf{w}_k \in \mathbb{C}^{NL \times 1}$ is designed based on global channel estimates as

$$\mathbf{w}_{k} = \left[\mathbf{a}_{k,1} \mathbf{w}_{k,1}^{\mathrm{T}}, ..., \mathbf{a}_{k,L} \mathbf{w}_{k,L}^{\mathrm{T}}\right]^{\mathrm{T}} = \sqrt{\rho_{k}} \frac{\overline{\mathbf{w}}_{k}}{\sqrt{\mathbb{E}_{\widehat{\mathbf{h}}} \{\|\overline{\mathbf{w}}_{k}\|^{2}\}}}, \quad (8)$$

where $\overline{\mathbf{w}}_k \in \mathbb{C}^{NL \times 1}$ defines the direction of the collective precoding vector. Moreover, ρ_k is the power globally allocated to the UE k, and $\mathbb{E}_{\widehat{\mathbf{h}}}\{\|\mathbf{w}_k\|^2\} = \rho_k$. We adopt the partial MMSE (P-MMSE) for the centralized processing, and employ the MR and local partial MMSE (LP-MMSE) precoding for the distributed processing. These schemes are chosen due to their scalability properties [3]. The MR scheme is implemented by setting $\overline{\mathbf{w}}_{k,l} = \mathbf{h}_{k,l}$ in (7). This precoding technique has low computational complexity, maximizes the received signal power at the UE using only the local CSI, but does not mitigate the multi-user interference. Whereas, the LP-MMSE precoding scheme suppresses interference only from the UEs served by each AP, relying solely on locally available channel estimates. While it is more complex than the MR scheme, it can yield better SE performance. The LP-MMSE precoding vector, from AP l to UE $k \in \mathcal{K}_l$, is given by [3]

$$\overline{\mathbf{w}}_{k,l}^{\text{LP-MMSE}} = \eta_k \left(\sum_{i \in \mathcal{K}_l} \eta_i \left(\widehat{\mathbf{h}}_{i,l} \widehat{\mathbf{h}}_{i,l}^{\text{H}} + \mathbf{U}_{i,l} \right) + \sigma_{\text{ul}}^2 \mathbf{I}_N \right)^{-1} \widehat{\mathbf{h}}_{k,l}, \quad (9)$$

where $\mathbf{U}_{i,l} = \mathbb{E}_{\widetilde{\mathbf{h}}}\{\widetilde{\mathbf{h}}_{i,l}\widetilde{\mathbf{h}}_{i,l}^{\mathrm{H}}\}$ is the correlation matrix of the estimation error $\widetilde{\mathbf{h}}_{i,l} = \mathbf{h}_{i,l} - \widehat{\mathbf{h}}_{i,l}$. The P-MMSE precoding scheme is used in centralized processing, and unlike MMSE

²The use of PSK modulation is motivated by the fact that DSTBC schemes are typically designed for unitary constellations. Moreover, since this paper aims to demonstrate the effectiveness of DSTBC in CF-mMIMO, PSK modulation is an appropriate choice. The use of rectangular constellations will be explored in future works.

does not consider all UEs' channel estimates for suppressing interference, but only the subset of UEs that most interfere with UE k, which is defined as $\mathcal{P}_k = \left\{i: \mathbf{a}_k \mathbf{a}_i^{\mathrm{H}} \neq \mathbf{0}_{L \times L}\right\}$. The P-MMSE precoding vector is given by

$$\overline{\mathbf{w}}_{k}^{\text{P-MMSE}} = \eta_{k} \left(\sum_{i \in \mathcal{P}_{k}} \eta_{i} \widehat{\mathbf{h}}_{i} \widehat{\mathbf{h}}_{i}^{\text{H}} + \mathbf{Z}_{\mathcal{P}_{k}} + \sigma_{\text{ul}}^{2} \mathbf{I}_{N} \right)^{-1} \widehat{\mathbf{h}}_{k}, \quad (10)$$

where $\hat{\mathbf{h}}_i = \left[\mathbf{a}_{i,1} \hat{\mathbf{h}}_{i,1}^\mathrm{T}, ..., \mathbf{a}_{i,L} \hat{\mathbf{h}}_{i,L}^\mathrm{T}\right]^\mathrm{T} \in \mathbb{C}^{NL \times 1}$ is the collective estimated channel vector and $\mathbf{Z}_{\mathcal{P}_k} = \sum_{i \in \mathcal{P}_k} \eta_i \mathbf{U}_i$, with $\mathbf{U}_i = \operatorname{diag}(\mathbf{a}_{i,1}\mathbf{U}_{i,1}, ..., \mathbf{a}_{i,L}\mathbf{U}_{i,L}).$

Two scalable power allocation strategies are considered in this work. For the centralized processing, we adopt the fractional power allocation,³ as it preserves the ability to mitigate the multi-user interference. The power coefficient ρ_k is computed as [3], [30]

$$\rho_{k} = \rho_{\max} \frac{\left(\sum_{l \in \mathcal{M}_{k}} \beta_{k,l}^{\varsigma}\right)^{\kappa} \varpi_{k}^{-\zeta}}{\max_{\ell \in \mathcal{M}_{k}} \sum_{i \in \mathcal{K}_{\ell}} \left(\sum_{l \in \mathcal{M}_{i}} \beta_{i,l}^{\varsigma}\right)^{\kappa} \varpi_{i}^{1-\zeta}}, \quad (11)$$

where $\beta_{k,l} = \operatorname{tr}\{\mathbf{R}_{k,l}\}/N$ denotes the large-scale fading coefficients of the UE k to the AP l. The term ϖ_k represents the largest fraction of ρ_k that can be allocated to a single AP serving the UE k, i.e., $\varpi_k = \max_{\ell \in \mathcal{M}_k} \mathbb{E}_{\widehat{\mathbf{h}}} \{ \|\bar{\mathbf{w}}_{k,\ell}\|^2 \}$. Moreover, $\zeta \in [-1,1]$, $\kappa \in [0,1]$, and ς are design parameters. For the distributed processing, the power is allocated proportionally to the large-scale fading gains of each UE, as proposed in [29]. Accordingly, $\rho_{k,l}, k \in \mathcal{K}_l$, is given by

$$\rho_{k,l} = \rho_{\max} \frac{\sqrt{\beta_{k,l}}}{\sum_{i \in \mathcal{K}_l} \sqrt{\beta_{i,l}}} \,. \tag{12}$$

D. Spectral Efficiency

In UC CF-mMIMO systems, although the capacity bounds implicitly account for phase misalignment effects, they do not clearly reveal how much the SE degrades as the value of θ_l increases. This is because the oscillators' phases vary independently across APs and fluctuate over time, impairing the characterization of the SE as an explicit function of ϑ_l . To overcome this analytical limitation, this paper incorporates the statistical characterization of oscillator phase variations into the SE analysis. The expected value of $e^{j\vartheta_l}$ is calculated as

$$\mathbb{E}_{\vartheta}\left\{e^{j\vartheta_{l}}\right\} = \frac{1}{2\alpha} \int_{-\alpha}^{\alpha} e^{j\vartheta_{l}} d\vartheta_{l} = \operatorname{sinc}\left(\alpha\right), \tag{13}$$

where the operator \mathbb{E}_{ϑ} indicates that the expectation is taken with respect to ϑ_l , $\forall l$. This result allows us to characterize the impact of phase misalignment on the DL SE of UC CF-mMIMO systems using two standard capacity bounds, which we refer to as achievable SEs. These capacity bounds will serve as the upper and lower performance limits of a UC CF-mMIMO system in our simulations. These capacity bounds are derived based on the signal model in (6).

Proposition 1: Assuming that the MMSE channel estimates are available at the APs, or at the CPU, and that the channel is perfectly known at the receiver, an upper bound⁴ on the achievable DL SE for UE k is given by

$$SE_{k}^{(\mathrm{dl},1)} = \frac{\tau_{d}}{\tau_{c}} \mathbb{E}_{\mathbf{h},\widehat{\mathbf{h}}} \left\{ \log_{2} \left(1 + SINR_{k}^{(\mathrm{dl},1)} \right) \right\}, \tag{14}$$

where the expectations $\mathbb{E}_{\mathbf{h}|\widehat{\mathbf{h}}}$ are computed with respect to the true and estimated channel realizations. The term au_d/ au_c is the fraction of samples per coherence block dedicated to transmitting the DL data. Furthermore, $SINR_k^{(dl,1)}$ represents the DL instantaneous effective SINR, which is given by

$$\operatorname{SINR}_{k}^{(\operatorname{dl},1)} = \frac{\mathbb{E}_{\vartheta} \left\{ \left| \sum_{l=1}^{L} e^{j\vartheta_{l}} \mathbf{h}_{k,l}^{(\operatorname{ef})} \right|^{2} \right\}}{\sum_{i=1, i \neq k}^{K} \mathbb{E}_{\vartheta} \left\{ \left| \sum_{l=1}^{L} e^{j\vartheta_{l}} \widetilde{\mathbf{h}}_{i,k,l}^{(\operatorname{ef})} \right|^{2} \right\} + \sigma_{\operatorname{dl}}^{2}}, \quad (15)$$

and where $\mathbf{h}_{k,l}^{(\mathrm{ef})} = \mathbf{a}_{k,l} \mathbf{h}_{k,l}^{\mathrm{H}} \mathbf{w}_{k,l}$, and $\widetilde{\mathbf{h}}_{i,k,l}^{(\mathrm{ef})} = \mathbf{a}_{i,l} \mathbf{h}_{k,l}^{\mathrm{H}} \mathbf{w}_{i,l}$.

Proof: This result readily follows from utilizing [3, Lemma 3.5] on the signal model in (6) while taking the statistical expectation with respect to $\{\vartheta_I\}$.

To write (15) as a function of the average value of the oscillator phases at each AP, we reformulate the numerator, respectively, the expectation in the denominator of (15) as

$$\sum_{l=1}^{L} \sum_{l'=1}^{L} \mathbb{E}_{\vartheta} \left\{ e^{j(\vartheta_{l} - \vartheta_{l'})} \right\} \mathbf{h}_{k,l}^{(\text{ef})} \mathbf{h}_{k,l'}^{(\text{ef})*}, \qquad (16)$$

$$\sum_{l=1}^{L} \sum_{l'=1}^{L} \mathbb{E}_{\vartheta} \left\{ e^{j(\vartheta_{l} - \vartheta_{l'})} \right\} \widetilde{\mathbf{h}}_{i,k,l}^{(\text{ef})} \widetilde{\mathbf{h}}_{i,k,l'}^{(\text{ef})*}. \qquad (17)$$

$$\sum_{l=1}^{L} \sum_{l'=1}^{L} \mathbb{E}_{\vartheta} \left\{ e^{j(\vartheta_l - \vartheta_{l'})} \right\} \widetilde{\mathbf{h}}_{i,k,l}^{(\text{ef})} \widetilde{\mathbf{h}}_{i,k,l'}^{(\text{ef})*}. \tag{17}$$

Note that $\mathbb{E}_{\vartheta}\{e^{j(\vartheta_l-\vartheta_{l'})}\}=1$, if l=l', and $\mathbb{E}_{\vartheta}\{e^{j(\vartheta_l-\vartheta_{l'})}\}=\sin^2(\alpha)$, if $l\neq l'$. Hence, $\mathrm{SINR}_k^{(\mathrm{dl},1)}$ can be rewritten as

$$SINR_{k}^{(dl,1)} = \frac{\tilde{\nu} \left| \sum_{l=1}^{L} \mathbf{h}_{k,l}^{(ef)} \right|^{2} + (1 - \tilde{\nu}) \sum_{l=1}^{L} \left| \mathbf{h}_{k,l}^{(ef)} \right|^{2}}{\sum_{\substack{i=1\\i\neq k}}^{K} \left[\tilde{\nu} \left| \sum_{l=1}^{L} \widetilde{\mathbf{h}}_{i,k,l}^{(ef)} \right|^{2} + (1 - \tilde{\nu}) \sum_{l=1}^{L} \left| \widetilde{\mathbf{h}}_{i,k,l}^{(ef)} \right|^{2} \right] + \sigma_{dl}^{2}},$$
(18)

where $\tilde{\nu} = \mathrm{sinc}^2(\alpha)$. The impact of the phase misalignment on the DL SE can be easily inferred from (18) due to the decay behavior of the *sinc* function. For instance, when $\alpha = 0$, the resulting SINR corresponds to that of a fully coherent system, whereas for $\alpha = \pi$, it approaches the SINR of a fully non-coherent system. Moreover, deriving the SE in (14) in closed form is analytically not tractable due to the expectation operator outside the logarithm. However, it can be evaluated numerically via Monte Carlo simulations.

Proposition 2: When the MMSE channel estimates are available at the APs, or at the CPU, and the receiver has knowledge of the average effective channel, a lower bound on the achievable DL SE for UE k can be computed as

$$SE_k^{(dl,2)} = \frac{\tau_d}{\tau_c} \log_2 \left(1 + SINR_k^{(dl,2)} \right), \tag{19}$$

with $SINR_k^{(dl,2)}$ being computed in (20) shown at the top of the next page, where the operator $\mathbb{E}_{\mathbf{h},\vartheta}$ indicates that the

⁴In practice, the UE does not have access to perfect CSI, which may render the term achievable SE somewhat misleading under the aforementioned assumptions, particularly because the UE also lacks access to the phase misalignment of the APs. Nevertheless, in this paper, we use the term achievable SE to assess the full potential of a UC CF-mMIMO network under ideal conditions. In such a scenario, the SE is indeed achievable, allowing us to compute an upper bound that serves as an optimistic performance benchmark for conventional UC CF-mMIMO systems.

³A wide range of power allocation strategies has been proposed in the literature [3], [28], [29]. However, identifying the optimal scheme is beyond the scope of this paper.

$$SINR_{k}^{(dl,2)} = \frac{\left|\sum_{l=1}^{L} \mathbb{E}_{\mathbf{h},\vartheta} \left\{ e^{j\vartheta_{l}} \mathbf{h}_{k,l}^{(ef)} \right\} \right|^{2}}{\sum_{l=1}^{K} \sum_{i\neq k} \mathbb{E}_{\mathbf{h},\vartheta} \left\{ \left|\sum_{l=1}^{L} e^{j\vartheta_{l}} \widetilde{\mathbf{h}}_{i,k,l}^{(ef)} \right|^{2} - \left|\sum_{l=1}^{L} \mathbb{E}_{\mathbf{h},\vartheta} \left\{ e^{j\vartheta_{l}} \mathbf{h}_{k,l}^{(ef)} \right\} \right|^{2} + \sigma_{dl}^{2}}$$
(20)

expectations are taken over both the channel realizations and the phase misalignments.

Proof: This result readily follows from utilizing [3, Corollary 6.3] on the signal model in (6) while taking the statistical expectation with respect to $\{\vartheta_l\}$ as well.

Equation (20) is also known as the *hardening bound*, which is a typical capacity lower bound utilized in massive MIMO theory that is valid for any choice of precoding vector. To characterize the impacts of phase misalignment in (20), we rely on the fact that $e^{j\vartheta_l}$ is statistically independent of the channel. Then, by following a similar procedure to that used in the derivation of (18), (20) can be reformulated as in (21) shown at the top of the next page.

Corollary 1: By using the MR precoding scheme with $\overline{\mathbf{w}}_{k,l} = \widehat{\mathbf{h}}_{k,l}$ in (7), $\mathbb{E}_{\mathbf{h}} \left\{ \mathbf{h}_{k,l}^{(\mathrm{ef})} \right\}$ in (21) becomes [3]

$$\mathbb{E}_{\mathbf{h}}\left\{\mathbf{h}_{k,l}^{(\text{ef})}\right\} = \sqrt{\eta_k \tau_p \rho_{k,l} \operatorname{tr}(\mathbf{a}_{k,l} \mathbf{\Theta}_{k,l})},\tag{22}$$

with $\Theta_{k,l} = \mathbf{R}_{k,l} \mathbf{\Psi}_{q_k,l}^{-1} \mathbf{R}_{k,l}$. $\mathbb{E}_{\mathbf{h}} \left\{ \left| \sum_{l=1}^{L} \widetilde{\mathbf{h}}_{i,k,l}^{(ef)} \right|^{2} \right\}$ is given by $\mathbb{E}_{\mathbf{h}} \left\{ \left| \sum_{l=1}^{L} \widetilde{\mathbf{h}}_{i,k,l}^{(ef)} \right|^{2} \right\} = \sum_{l=1}^{L} \rho_{i,l} \frac{\operatorname{tr}(\mathbf{a}_{i,l} \mathbf{\Theta}_{i,l} \mathbf{R}_{k,l})}{\operatorname{tr}(\mathbf{\Theta}_{i,l})}$ $+ \left| \sum_{l=1}^{L} \sqrt{\frac{\eta_{k} \tau_{p} \rho_{i,l}}{\operatorname{tr}(\mathbf{\Theta}_{i,l})}} \operatorname{tr}(\mathbf{a}_{i,l} \widetilde{\mathbf{\Theta}}_{i,k,l}) \right|^{2} \mathbb{I}_{i,k}, \tag{23}$

where $\widetilde{\Theta}_{i,k,l} = \mathbf{R}_{i,l} \mathbf{\Psi}_{q_i,l}^{-1} \mathbf{R}_{k,l}$ and the binary indicator $\mathbb{I}_{i,k} \in \{0,1\}$ specifies the UEs sharing the same pilot signal, with $\mathbb{I}_{i,k} = 1$ corresponding to $i \in \mathcal{Q}_k$, and $\mathbb{I}_{i,k} = 0$ otherwise. Besides, the expectations $\mathbb{E}_{\mathbf{h}} \{ |\widetilde{\mathbf{h}}_{i,k,l}^{(\text{ef})}|^2 \}$ are obtained as

$$\mathbb{E}_{\mathbf{h}}\left\{\left|\widetilde{\mathbf{h}}_{i,k,l}^{(\mathrm{ef})}\right|^{2}\right\} = \rho_{i,l} \frac{\operatorname{tr}(\mathbf{a}_{i,l}\boldsymbol{\Theta}_{i,l}\mathbf{R}_{k,l})}{\operatorname{tr}(\boldsymbol{\Theta}_{i,l})} + \left|\sqrt{\frac{\eta_{k}\tau_{p}\rho_{i,l}}{\operatorname{tr}(\boldsymbol{\Theta}_{i,l})}} \operatorname{tr}(\mathbf{a}_{i,l}\widetilde{\boldsymbol{\Theta}}_{i,k,l})\right|^{2} \mathbb{I}_{i,k}.$$
(24)

Proof: The closed-form expressions for the expectations associated with $\mathbb{E}_{\mathbf{h}} \big\{ \sum_{l=1}^L \big| \widetilde{\mathbf{h}}_{i,k,l}^{(\mathrm{ef})} \big|^2 \big\}$ can be computed by leveraging the properties of jointly Gaussian vectors [3, Lemma B.5]. That is, given two circularly-symmetric complex normals vectors $\widetilde{\mathbf{x}}$ and $\widetilde{\mathbf{y}}$, $\mathbb{E} \big\{ \big| \widetilde{\mathbf{x}}^{\mathrm{H}} \widetilde{\mathbf{y}} \big|^2 \big\}$ is calculated as

$$\operatorname{tr}\left(\mathbb{E}\left\{\widetilde{\mathbf{x}}\widetilde{\mathbf{x}}^{\mathrm{H}}\right\}\mathbb{E}\left\{\widetilde{\mathbf{y}}\widetilde{\mathbf{y}}^{\mathrm{H}}\right\}\right) + \left|\operatorname{tr}\left(\mathbb{E}\left\{\widetilde{\mathbf{y}}\widetilde{\mathbf{x}}^{\mathrm{H}}\right\}\right)\right|^{2}.$$
 (25)

By setting $\overline{\mathbf{w}}_{i,l} = \widehat{\mathbf{h}}_{i,l}$ in (7), one can compute

$$\widetilde{\mathbf{h}}_{i,k,l}^{(\text{ef})} = \mathbf{a}_{i,l} \sqrt{\rho_{i,l}} \mathbf{h}_{k,l}^{\text{H}} \widehat{\mathbf{h}}_{i,l} / \sqrt{\mathbb{E}_{\mathbf{h}} \{ \| \widehat{\mathbf{h}}_{i,l} \|^2 \}}.$$
 (26)

Let us define the vectors $\widetilde{\mathbf{x}}$ and $\widetilde{\mathbf{y}}$ as $\widetilde{\mathbf{x}} = \mathbf{a}_{i,l} \sqrt{\rho_{i,l}} \mathbf{h}_{k,l}^{\mathrm{H}}$ and $\widetilde{\mathbf{y}} = \widehat{\mathbf{h}}_{i,l} / \sqrt{\mathbb{E}_{\mathbf{h}} \{ \|\widehat{\mathbf{h}}_{i,l}\|^2 \}}$. By applying $\widetilde{\mathbf{x}}$ and $\widetilde{\mathbf{y}}$ in (25), we obtain $\mathbb{E}_{\mathbf{h}} \{ |\widetilde{\mathbf{h}}_{i,k,l}^{(\mathrm{ef})}|^2 \}$ as in (24).

III. DL DATA TRANSMISSION RESILIENT TO PHASE MISALIGNMENT EFFECTS

The concept of DSTBC was introduced in MIMO systems as an extension of STBC schemes. Its aim is to enhance trans-

mission diversity by leveraging the multiple antennas at the transmitter and potentially at the receiver. More specifically, DSTBC techniques serve as the differential counterpart of space-time block coding, with the key distinction that they do not require CSI knowledge at the receiver. More precisely, in our proposed scheme, the channel estimates are used at the network side to compute the precoding vectors $\mathbf{w}_{k,l}$ for all APs serving the UE k aimed at suppressing multiuser interference; however, the detection scheme does not need such knowledge.

A. Differential Transmission

Differential transmission in DSTBC methods involves splitting the data symbols for the UE into several space-time codewords. The receiver decodes the data by analyzing two consecutive received codewords, also called received signal blocks. To explain this process: consider the UE k which is supported by L_k APs, where $L_k = |\mathcal{M}_k|$. Let P denote the number of symbols periods that a space-time codeword encompasses, and let $\mathcal{S}_k = \{s_k^1, s_k^2, \dots, s_k^{N_{sym}}\}$ be the set of N_{sym} complex information symbols selected from a unitary constellation for the UE k. This set, S_k , is divided by the CPU into smaller groups, each containing n_s complex symbols. The number of these subsets in S_k is represented by G, which is calculated as $G = \lfloor \tau_d/P \rfloor$. Furthermore, the t-th subset of \mathcal{S}_k is defined as $\mathcal{S}_k^t = \{s_k^{(t-1)n_s+1}, \ldots, s_k^{tn_s}\}$, with the cardinality of \mathcal{S}_k^t being equal to $|\mathcal{S}_k^t| = n_s$. Then, each subset \mathcal{S}_k^t is mapped by the CPU onto a code matrix $\mathbf{X}_k^t \in \mathbb{C}^{L_k \times P}$, where t also denotes the index of the code matrix. To facilitate detection, \mathbf{X}_k^t is typically designed as a unitary matrix, i.e., $\mathbf{X}_k^t(\mathbf{X}_k^t)^{\mathrm{H}} = \mathbf{I}_{L_k}$. In addition, these matrices are often designed to be orthogonal, meaning that the inner product between distinct rows of \mathbf{X}_k^t is zero. The orthogonality property further contributes to reducing the detection complexity at the receiver. Nonetheless, orthogonal STBC matrices possess only a semi-unitary structure. In particular, the product $\mathbf{X}_k^t(\mathbf{X}_k^t)^{\mathrm{H}}$ results in $\mathbf{X}_k^t(\mathbf{X}_k^t)^{\mathrm{H}} = \sum_{n=1}^{n_s} \left| s_k^n \right|^2 \mathbf{I}_{L_k}$. To transform \mathbf{X}_k^t into a unitary matrix, \mathbf{X}_k^t it is typically scaled by a factor of $1/\sqrt{n_s}$, which yields to

$$\mathbf{X}_{k}^{t}(\mathbf{X}_{k}^{t})^{\mathrm{H}} = \frac{1}{n_{s}} \sum_{n=1}^{n_{s}} \left| s_{k}^{n} \right|^{2} \mathbf{I}_{L_{k}} = \mathbf{I}_{L_{k}},$$
 (27)

provided that s_k^n is taken from a unitary constellation, i.e., $|s_k^n| = 1$. For simplicity, this paper also focuses on square code matrices, i.e., by assuming $P = L_k$.

Example (Orthogonal Code Matrices): A well-established orthogonal code matrix in the literature is the Alamouti matrix, which encodes two complex symbols $(n_s = 2)$ over two symbol periods (P = 2), resulting in a code rate of $R = n_s/P = 1$. For instance, when t = 1, the Alamouti matrix is expressed as

$$\mathbf{X}_{k}^{t} = \frac{1}{\sqrt{2}} \begin{bmatrix} s_{k}^{1} & (s_{k}^{2})^{*} \\ s_{k}^{2} & -(s_{k}^{1})^{*} \end{bmatrix}. \tag{28}$$

One can note that s_k^1 and s_k^2 are the two consecutive elements of S_k^t for t = 1. For t > 1, (28) would involve the symbols from

$$SINR_{k}^{(dl,2)} = \frac{\tilde{\nu} \left| \sum_{l=1}^{L} \mathbb{E}_{\mathbf{h}} \left\{ \mathbf{h}_{k,l}^{(ef)} \right\} \right|^{2}}{\sum_{i=1, i \neq k}^{K} \mathbb{E}_{\mathbf{h}} \left\{ \tilde{\nu} \left| \sum_{l=1}^{L} \widetilde{\mathbf{h}}_{i,k,l}^{(ef)} \right|^{2} + (1 - \tilde{\nu}) \sum_{l=1}^{L} \left| \widetilde{\mathbf{h}}_{i,k,l}^{(ef)} \right|^{2} \right\} - \tilde{\nu} \left| \sum_{l=1}^{L} \mathbb{E}_{\mathbf{h}} \left\{ \mathbf{h}_{k,l}^{(ef)} \right\} \right|^{2} + \sigma_{dl}^{2}}$$
(21)

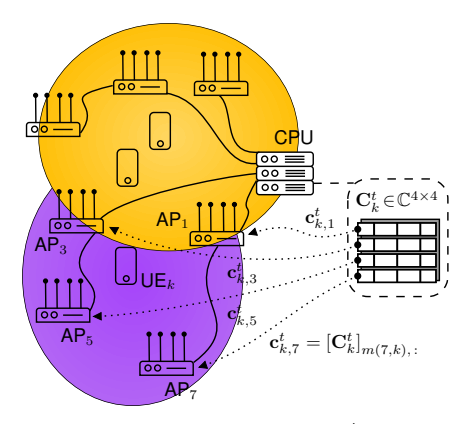


Fig. 1: Illustration of how the information matrix \mathbf{C}_k^t is row-wise split among the APs serving UE k. The CPU assigns each row of matrix $\mathbf{C}_k^t \in \mathbb{C}^{L_k \times L_k}$ to an AP serving the UE k via the mapping m(l,k), with $l \in \mathcal{M}_k$. In this illustration, a matrix of dimension $\mathbf{C}_k^t \in \mathbb{C}^{4 \times 4}$ is considered. Thus, \mathbf{C}_k^t is composed of four rows, each comprising a duration time of four symbols. To exemplify the meaning of the mapping m(l,k), note that, since AP 7 is assigned the fourth row of \mathbf{C}_k^t , it follows that m(7,k)=4.

the corresponding subset S_k^t . For instance, when t=2, the elements of (28) correspond to s_k^3 and s_k^4 . For configurations with a higher number of APs serving the UE, other orthogonal matrices exist; as an example, if $L_k=4$, the following orthogonal code matrix can be employed

$$\mathbf{X}_{k}^{t} = \frac{1}{\sqrt{3}} \begin{bmatrix} s_{k}^{1} & 0 & s_{k}^{2} & -s_{k}^{3} \\ 0 & s_{k}^{1} & (s_{k}^{3})^{*} & (s_{k}^{2})^{*} \\ -(s_{k}^{2})^{*} & -s_{k}^{3} & (s_{k}^{1})^{*} & 0 \\ (s_{k}^{3})^{*} & -s_{k}^{2} & 0 & (s_{k}^{1})^{*} \end{bmatrix}, \quad (29)$$

where (29) contains the elements of S_k^t for t = 1. This code matrix sends $n_s = 3$ symbols over P = 4 symbol periods, thus having the code rate of R = 3/4.

Once defined the code matrices, the CPU encodes \mathbf{X}_k^t differentially by forming the matrix $\mathbf{C}_k^t \in \mathbb{C}^{L_k \times L_k}$, given by

$$\mathbf{C}_k^t = \mathbf{C}_k^{t-1} \mathbf{X}_k^t. \tag{30}$$

 \mathbf{C}_k^t conveys the information signal to be transmitted to the UE k, with $\mathbf{C}_k^0 = \mathbf{I}_{L_k}$. Given that \mathbf{X}_k^t is a unitary matrix, the matrix \mathbf{C}_k^t is also unitary, i.e., $\mathbf{C}_k^t(\mathbf{C}_k^t)^{\mathrm{H}} = \mathbf{I}_{L_k}$. However, note that (30) cannot be directly transmitted to the UE k. Recall that the UE k is served by L_k APs, whose indices may range from 1 to L. Meanwhile, the row indices of \mathbf{C}_k^t span from 1 to L_k , which may not directly correspond to the indices of the APs serving the UE k, as L_k is typically smaller than L. Hence, before transmitting \mathbf{C}_k^t to UE k, the CPU distributes the rows of \mathbf{C}_k^t among the APs serving the UE k, i.e., for all AP l in \mathcal{M}_k . The row of \mathbf{C}_k^t assigned to AP l is [1]

$$\mathbf{c}_{k,l}^t = \left[\mathbf{C}_k^{t-1}\right]_{m(l,k),:} \mathbf{X}_k^t, \tag{31}$$

where $l \in \mathcal{M}_k$ and $m(l,k) \in \{1,...,L_k\}$ is a mapping function that assigns a specific row of the matrix \mathbf{C}_k^t to AP l (see Fig. 1 for a graphical example). Let $\sum_{k=1}^K \mathbf{a}_{k,l} \mathbf{w}_{k,l} \mathbf{c}_{k,l}^t \in \mathbb{C}^{N \times L_k}$ represent the signal sent by AP l. The received signal block

can be expressed as

$$\mathbf{y}_{k}^{t} = \sum_{l=1}^{L} \mathbf{g}_{k,l}^{(\text{ef})} \left[\mathbf{C}_{k}^{t-1} \right]_{m(l,k),:} \mathbf{X}_{k}^{t} + \widetilde{\mathbf{n}}_{k}^{t}, \tag{32}$$

where $\mathbf{g}_{k,l}^{(\mathrm{ef})} \left[\mathbf{C}_k^{t-1} \right]_{m(l,k),:}$ is unknown at the UE k. Moreover, $\widetilde{\mathbf{n}}_k^t$ denotes the combined effects of interference and receiver noise, being given by

$$\widetilde{\mathbf{n}}_{k}^{t} = \sum_{i=1, i \neq k}^{K} \sum_{l=1}^{L} \widetilde{\mathbf{g}}_{i,k,l}^{(ef)} \left[\mathbf{C}_{i}^{t-1} \right]_{m(l,i),:} \mathbf{X}_{i}^{t} + \mathbf{n}_{k}^{t}, \qquad (33)$$

where $\mathbf{n}_k^t \sim \mathcal{N}_{\mathbb{C}}(\mathbf{0}, \sigma_{\mathrm{dl}}^2 \mathbf{I}_{L_k})$ represents the receiver noise.

B. Differential Detection

The code matrix \mathbf{X}_k^t can be decoded by using two consecutive received blocks, i.e., \mathbf{y}_k^t and \mathbf{y}_k^{t-1} , where \mathbf{y}_k^{t-1} is given by $\mathbf{y}_k^{t-1} = \sum_{l=1}^L \mathbf{g}_{k,l}^{(\mathrm{ef})} \left[\mathbf{C}_k^{t-1} \right]_{m(l,k),:} + \widetilde{\mathbf{n}}_k^{t-1}$, and with $\widetilde{\mathbf{n}}_k^{t-1} = \sum_{i=1,i\neq k}^K \sum_{l=1}^L \widetilde{\mathbf{g}}_{i,k,l}^{(\mathrm{ef})} \left[\mathbf{C}_i^{t-1} \right]_{m(l,i),:} + \mathbf{n}_k^{t-1}$. The ML detection of \mathbf{X}_k^t corresponds to compute [26]

$$\hat{\mathbf{X}}_{k}^{t} = \underset{\mathbf{X} \in \mathcal{X}_{N}}{\operatorname{arg\,min}} - 2\operatorname{Re}\left\{\operatorname{tr}\left\{\mathbf{X}\left(\mathbf{y}_{k}^{t}\right)^{\operatorname{H}}\mathbf{y}_{k}^{t-1}\right\}\right\} + \operatorname{const}, (34)$$

or equivalently $\hat{\mathbf{X}}_k^t = \arg\max_{\mathbf{X} \in \mathcal{X}_N} \operatorname{Re}\{\operatorname{tr}\{\mathbf{X} \left(\mathbf{y}_k^t\right)^{\operatorname{H}} \mathbf{y}_k^{t-1}\}\}$, where \mathcal{X}_N represents the set of all possible code matrices for a given unitary constellation \mathcal{S} . The detection of $\hat{\mathbf{X}}_k^t$ in (34) can be computationally intensive as it involves an exhaustive search over all possible codewords $\mathbf{X} \in \mathcal{X}_N$. Nonetheless, the detection complexity can be significantly reduced if the codewords belonging to \mathcal{X}_N are designed as orthogonal code matrices, as previously mentioned. This is because orthogonal code matrices allow the ML detection of the symbols in \mathbf{X}_k^t to be decoupled. Consequently, each symbol can be detected individually rather than jointly detecting the entire code matrix. To facilitate data detection, a generic codeword \mathbf{X} is redefined as

$$\mathbf{X} = \frac{1}{\sqrt{n_s}} \sum_{n=1}^{n_s} \bar{s}^n \mathbf{A}_n + j \tilde{s}^n \mathbf{B}_n, \tag{35}$$

where the complex symbol $s^n \in \mathcal{S}$ is composed of its real and imaginary parts \bar{s}^n , \tilde{s}^n , such that $s^n = \bar{s}^n + j\tilde{s}^n$. Moreover, the matrices $\mathbf{A}_n \in \mathbb{Z}^{L_k \times L_k}$ and $\mathbf{B}_n \in \mathbb{Z}^{L_k \times L_k}$ are referred to as *amicable orthogonal designs*, which consist of a set of predefined matrices that satisfy the following conditions

$$\mathbf{A}_{n}\mathbf{A}_{n}^{\mathrm{H}} = \mathbf{I}_{L_{k}}, \qquad \mathbf{B}_{n}\mathbf{B}_{n}^{\mathrm{H}} = \mathbf{I}_{L_{k}},$$

$$\mathbf{A}_{n}\mathbf{A}_{n'}^{\mathrm{H}} = -\mathbf{A}_{n'}\mathbf{A}_{n}^{\mathrm{H}}, \quad \mathbf{B}_{n}\mathbf{B}_{n'}^{\mathrm{H}} = -\mathbf{B}_{n'}\mathbf{B}_{n}^{\mathrm{H}}, \quad n \neq n',$$

$$\mathbf{A}_{n}\mathbf{B}_{n'}^{\mathrm{H}} = \mathbf{B}_{n'}\mathbf{A}_{n}^{\mathrm{H}}.$$
(36)

with n and n' being the indices that identify different matrices. The number of distinct matrices in sets $\{\mathbf{A}_n\}_{n=1}^{n_s}$ and $\{\mathbf{B}_n\}_{n=1}^{n_s}$ is n_s for each set. For instance, for the Alamouti code $(n_s=2)$, these sets are defined as

$$\mathbf{A}_{1} = \begin{bmatrix} 1 & 0 \\ 0 & -1 \end{bmatrix}, \quad \mathbf{B}_{1} = \begin{bmatrix} 1 & 0 \\ 0 & 1 \end{bmatrix},$$

$$\mathbf{A}_{2} = \begin{bmatrix} 0 & 1 \\ 1 & 0 \end{bmatrix}, \quad \mathbf{B}_{2} = \begin{bmatrix} 0 & -1 \\ 1 & 0 \end{bmatrix}.$$

$$(37)$$

For other code matrices, like the one in (29), there are additional unique sets of amicable orthogonal designs.⁵

Once the set of amicable orthogonal designs is defined, we can substitute (35) into (34). Then, we obtain a ML criterion that can be minimized with respect to each symbol s^n belonging to the unitary constellation $\mathcal{S}.$ Let $s_k^{\widetilde{m}(n,t)}\subset \mathcal{S}_k^t$ denote the n-th complex symbol among the n_s symbols transmitted within the code matrix \mathbf{X}_k^t , for $n=1,\ldots,n_s.$ Specifically, $s_k^{\widetilde{m}(n,t)}$ is one of the symbols belonging to the subset \mathcal{S}_k^t , defined as $\mathcal{S}_k^t=s_k^{(t-1)n_s+1},\ldots,s_k^{tn_s}.$ Here, $\widetilde{m}(n,t)$ is a mapping function that associates the value of n to the corresponding position of $s_k^{\widetilde{m}(n,t)}$ in $\mathcal{S}_k^t.$ For instance, n=1 indicates that $s_k^{\widetilde{m}(n,t)}$ corresponds to $s_k^{(t-1)n_s+1},$ whereas $n=n_s$ refers to $s_k^{tn_s}.$ Let us define

$$\mathbf{Y}_{k}^{t} = \left(\mathbf{y}_{k}^{t}\right)^{\mathbf{H}} \mathbf{y}_{k}^{t-1} \in \mathbb{C}^{L_{k} \times L_{k}}.$$
 (38)

The ML criterion used to detect $\hat{s}_k^{\widetilde{m}(n,t)}$ after substituting (35) into (34) is given by

$$\sum_{n=1}^{n_s} \left(-\operatorname{Re}\left\{\operatorname{tr}\left\{\mathbf{A}_n \mathbf{Y}_k^t\right\}\right\} \bar{s}^n + \operatorname{Im}\left\{\operatorname{tr}\left\{\mathbf{B}_n \mathbf{Y}_k^t\right\}\right\} \tilde{s}^n\right).$$
(39)

It can be noted that the ML metric in (34) decouples into a sum of n_s terms in (39), each involving exactly one complex symbol. Consequently, the detection of $\hat{s}_k^{\widetilde{m}(n,t)}$ is decoupled from the detection of $\hat{s}_k^{\widetilde{m}(n',t)}$, for $n \neq n'$. Therefore, the complex symbol $\hat{s}_k^{\widetilde{m}(n,t)}$ can also be detected by

$$\underset{s^n \in \mathcal{S}}{\arg\min} - \operatorname{Re}\left\{\operatorname{tr}\left\{\mathbf{A}_n \mathbf{Y}_k^t\right\}\right\} \bar{s}^n + \operatorname{Im}\left\{\operatorname{tr}\left\{\mathbf{B}_n \mathbf{Y}_k^t\right\}\right\} \tilde{s}^n, \tag{40}$$

where the detected symbol $\hat{s}_k^{\widetilde{m}(n,t)}$ is composed of its real and imaginary parts, $\bar{\hat{s}}_k^{\widetilde{m}(n,t)}$ and $\tilde{\hat{s}}_k^{\widetilde{m}(n,t)}$, respectively. Thus, the product $\operatorname{Re}\{\operatorname{tr}\{\mathbf{A}_n\,\mathbf{Y}_k^t\}\}\bar{s}^n$ is used to detect $\bar{\hat{s}}_k^{\widetilde{m}(n,t)}$, while $\operatorname{Im}\{\operatorname{tr}\{\mathbf{B}_n\,\mathbf{Y}_k^t\}\}\tilde{s}^n$ is utilized to detect $\tilde{\hat{s}}_k^{\widetilde{m}(n,t)}$.

C. Resilience to Phase Misalignment Effects and SNR

Let us consider the decision statistic related to \bar{s}^n in (40), and let $\mathbf{DS}_k^t = \sum_{l=1}^L \mathbf{g}_{k,l}^{(\mathrm{ef})} \left[\mathbf{C}_k^t \right]_{m(l,k),:} \in \mathbb{C}^{1 \times L_k}$ denote the desired signal of UE k for the received signal block \mathbf{y}_k^t , where the last equality, i.e., $\left[\mathbf{C}_k^t \right]_{m(l,k),:} = \left[\mathbf{C}_k^{t-1} \right]_{m(l,k),:} \mathbf{X}_k^t$, comes from (31). Then, by considering the single-user case, we can write \mathbf{y}_k^t and \mathbf{y}^{t-1} as $\mathbf{y}_k^t = \mathbf{DS}_k^t + \mathbf{n}_k^t$ and $\mathbf{y}_k^{t-1} = \mathbf{DS}_k^{t-1} + \mathbf{n}_k^{t-1}$. Recall from (38) that $\mathbf{Y}_k^t = (\mathbf{y}_k^t)^H \mathbf{y}_k^{t-1}$. By letting $\mathbf{ML}_{k,n}^t$ denote $\mathrm{tr}\{\mathbf{A}_n\,\mathbf{Y}_k^t\}$ in (40), we obtain an expression consisting of four distinct terms, i.e.,

$$ML_{k,n}^t = ML_{k,n,1}^t + ML_{k,n,2}^t + ML_{k,n,3}^t + ML_{k,n,4}^t,$$
 (41)

where $\mathrm{ML}_{k,n,1}^t = \mathbf{A}_n \big(\mathbf{D}\mathbf{S}_k^t\big)^\mathrm{H} \mathbf{D}\mathbf{S}_k^{t-1}$. Thus,

$$\mathbf{ML}_{k,n,1}^{t} = \sum_{l=1}^{L} \sum_{l'=1}^{L} \operatorname{tr} \left\{ \mathbf{g}_{k,l}^{(\text{ef})H} \mathbf{g}_{k,l'}^{(\text{ef})} \mathbf{A}_{n} \left(\mathbf{X}_{k}^{t} \right)^{H} \mathbf{C}_{k,m,m',l,l'}^{t-1,t-1} \right\}, (42)$$

with $\mathbf{C}_{k,m,m',l,l'}^{t-1,t-1} = \left[\mathbf{C}_{k}^{t-1}\right]_{m(l,k),:}^{\mathbf{H}} \left[\mathbf{C}_{k}^{t-1}\right]_{m'(l',k),:}^{\mathbf{H}}$. The term $\mathbf{ML}_{k,n,2}^{t} = \mathbf{A}_{n} {\left(\mathbf{n}_{k}^{t}\right)}^{\mathbf{H}} \mathbf{DS}_{k}^{t-1}$ is obtained as

$$ML_{k,n,2}^{t} = \sum_{l=1}^{L} \text{tr} \{ g_{k,l}^{(\text{ef})} \mathbf{A}_{n} (\mathbf{n}_{k}^{t})^{H} [\mathbf{C}_{k}^{t-1}]_{m(l,k),:} \}, \quad (43)$$

⁵We omit details in this regard due to space constraints. The methodology for generating amicable orthogonal designs can be found in [26].

whereas $\mathrm{ML}_{k,n,3}^t = \mathbf{A}_n \big(\mathbf{D}\mathbf{S}_k^t\big)^{\mathrm{H}} \mathbf{n}_k^{t-1}$ is given by

$$\mathrm{ML}_{k,n,3}^{t} = \sum_{l=1}^{L} \mathrm{tr} \left\{ \mathbf{g}_{k,l}^{(\mathrm{ef})\mathrm{H}} \mathbf{A}_{n} \left[\mathbf{C}_{k}^{t} \right]_{m(l,k),:}^{\mathrm{H}} \mathbf{n}_{k}^{t-1} \right\}, \tag{44}$$

with $\begin{bmatrix} \mathbf{C}_k^t \end{bmatrix}_{m(l,k),:} = \begin{bmatrix} \mathbf{C}_k^{t-1} \end{bmatrix}_{m(l,k),:} \mathbf{X}_k^t$, which can also be regarded as $\mathbf{c}_{k,l}^t$ in (31). The term $\mathrm{ML}_{k,n,4}^t$ is calculated as $\mathrm{ML}_{k,n,4}^t = \mathrm{tr} \big\{ \mathbf{A}_n \left(\mathbf{n}_k^t \right)^{\mathrm{H}} \mathbf{n}_k^{t-1} \big\}$. However, $\mathrm{ML}_{k,n,4}^t$ can be neglected if the noise variance σ_{dl}^2 is small enough.

To evaluate the SNR and assess the robustness of the proposed CF-mMIMO system using DSTBC schemes against phase misalignments, we begin by solving $\mathrm{ML}_{k,n,1}^t$. Hence, the code matrix $\left(\mathbf{X}_k^t\right)^{\mathrm{H}}$ in (42) is defined as

$$\left(\mathbf{X}_{k}^{t}\right)^{\mathrm{H}} = \frac{1}{\sqrt{n_{s}}} \sum_{n'=1}^{n_{s}} \bar{s}_{k}^{\widetilde{m}(n',t)} \mathbf{A}_{n'}^{\mathrm{H}} - j\tilde{s}_{k}^{\widetilde{m}(n',t)} \mathbf{B}_{n'}^{\mathrm{H}}.$$
 (45)

In the following, we split the computation of (42) into two steps. First, we evaluate (42) by considering the product $\mathbf{A}_n \left(\mathbf{X}_k^t \right)^{\mathrm{H}}$ without including the imaginary components of (45), i.e., without the term $-j \tilde{s}_k^{\tilde{m}(n',t)} \mathbf{B}_{n'}^{\mathrm{H}}$. Second, we indicate how to calculate the contributions of the imaginary terms of $\left(\mathbf{X}_k^t \right)^{\mathrm{H}}$ to $\mathrm{ML}_{k,n,1}^t$ in (42), as shown in Appendix A. To compute (42) without the imaginary components of (45), we define $\left(\overline{\mathbf{X}}_{k,n}^t \right)^{\mathrm{H}} = \mathrm{Re} \left\{ \mathbf{A}_n \left(\mathbf{X}_k^t \right)^{\mathrm{H}} \right\}$, which is given by

$$\left(\overline{\mathbf{X}}_{k,n}^{t}\right)^{\mathrm{H}} = \frac{1}{\sqrt{n_s}} \left(\overline{s}_k^{\widetilde{m}(n,t)} \mathbf{I}_{L_k} + \mathbf{E}_{k,n}^{t}\right),\tag{46}$$

where $\mathbf{E}_{k,n}^t$ is obtained as follows

$$\mathbf{E}_{k,n}^{t} = \sum_{n'=1,n'\neq n}^{n_s} \bar{s}_k^{\widetilde{m}(n',t)} \mathbf{A}_n \mathbf{A}_{n'}^{\mathrm{H}}.$$
 (47)

Given that (46) contains only real-valued terms, then

$$\overline{\mathrm{ML}}_{k,n,1}^{t} = \sum_{l=1}^{L} \sum_{l'=1}^{L} \mathrm{tr} \left\{ \mathbf{g}_{k,l}^{(\mathrm{ef})\mathrm{H}} \mathbf{g}_{k,l'}^{(\mathrm{ef})} \left(\overline{\mathbf{X}}_{k,n}^{t} \right)^{\mathrm{H}} \mathbf{C}_{k,m,m',l,l'}^{t-1,t-1} \right\}. (48)$$

Then, we split the cross-product terms in (48) into two cases: m(l,k)=m'(l',k) and $m(l,k)\neq m'(l',k)$. However, since (46) consists of two terms, i.e., $\bar{s}_k^{\widetilde{m}(n,t)}\mathbf{I}_{L_k}/\sqrt{n_s}$ and $\mathbf{E}_{k,n}^t/\sqrt{n_s}$, each case yields two contributions to $\overline{\mathrm{ML}}_{k,n,1}^t$, resulting in a total of four separate calculations. Let us begin by computing the contribution of $\bar{s}_k^{\widetilde{m}(n,t)}\mathbf{I}_{L_k}/\sqrt{n_s}$ to (48) for the case m(l,k)=m'(l',k). We denote this specific calculation as $\overline{\mathrm{ML}}_{k,n,1,1}^t$. By substituting $\bar{s}_k^{\widetilde{m}(n,t)}\mathbf{I}_{L_k}/\sqrt{n_s}$ in (48), the expression for $\overline{\mathrm{ML}}_{k,n,1,1}^t$ is obtained as

$$\overline{\mathrm{ML}}_{k,n,1,1}^{t} = \frac{\bar{s}_{k}^{\widetilde{m}(n,t)}}{\sqrt{n_{s}}} \sum_{l=1}^{L} g_{k,l}^{(\mathrm{ef}) \, \mathrm{H}} g_{k,l}^{(\mathrm{ef})} \mathrm{tr} \left\{ \mathbf{C}_{k,m,m,l,l}^{t-1,t-1} \right\}. \tag{49}$$

Recall that $\left[\mathbf{C}_{k}^{t-1}\right]_{m'(l',k),:}$ and $\left[\mathbf{C}_{k}^{t-1}\right]_{m(l,k),:}$ are row vectors. Given that $\mathbf{C}_{k,m,m',l,l'}^{t-1,t-1} = \left[\mathbf{C}_{k}^{t-1}\right]_{m(l,k),:}^{\mathbf{H}} \left[\mathbf{C}_{k}^{t-1}\right]_{m'(l',k),:}^{\mathbf{H}}$, and by applying the cyclic property of the trace, we obtain $\operatorname{tr}\left\{\mathbf{C}_{k,m,m',l,l'}^{t-1,t-1}\right\} = \left[\mathbf{C}_{k}^{t-1}\right]_{m'(l',k),:}^{\mathbf{H}} \left[\mathbf{C}_{k}^{t-1}\right]_{m(l,k),:}^{\mathbf{H}}$. Besides, since the information signal \mathbf{C}_{k}^{t-1} is assumed to be unitary and orthogonal, the following property holds

$$\operatorname{tr}\left\{\mathbf{C}_{k,m,m',l,l'}^{t-1,t-1}\right\} = \begin{cases} 1 & \text{for } m(l,k) = m'(l',k), \\ 0 & \text{for } m(l,k) \neq m'(l',k). \end{cases}$$
(50)

Consequently, (49) simplifies to

$$\overline{\mathrm{ML}}_{k,n,1,1}^{t} = \frac{1}{\sqrt{n_s}} \bar{s}_k^{\widetilde{m}(n,t)} \sum_{l=1}^{L} \left| \mathbf{g}_{k,l}^{(\mathrm{ef})} \right|^2. \tag{51}$$

Then, we compute the contribution of $\bar{s}_k^{\tilde{m}(n,t)}\mathbf{I}_{L_k}/\sqrt{n_s}$ to (48) in the case where $m(l,k) \neq m'(l',k)$. Let $\overline{\mathrm{ML}}_{k,n,1,3}^t$ denote this calculation. Accordingly, $\overline{\mathrm{ML}}_{k,n,1,3}^{\iota}$ is given by

$$\frac{\bar{s}_{k}^{\widetilde{m}(n,t)}}{\sqrt{n_{s}}} \sum_{l=1}^{L} \sum_{l'=1,l'\neq l}^{L} \mathbf{g}_{k,l}^{(\text{ef})\,\mathrm{H}} \mathbf{g}_{k,l'}^{(\text{ef})} \mathrm{tr} \left\{ \mathbf{C}_{k,m,m',l,l'}^{t-1,t-1} \right\} = 0, \quad (52)$$

as $\operatorname{tr}\left\{\mathbf{C}_{k,m,m',l,l'}^{t-1,t-1}\right\}=0$, for $m(l,k)\neq m'(l',k)$.

Lemma 1: The contributions of the remaining components, i.e., $\mathbf{E}_{k,n}^t$ and $-j\tilde{s}_k^{\widetilde{m}(n',t)}\mathbf{B}_{n'}^{\mathrm{H}}$, to the calculation of $\mathrm{ML}_{k,n,1}^t$ vanish when applying the real-part operation in (40). Thus,

$$\mathrm{ML}_{k,n,1}^t = \overline{\mathrm{ML}}_{k,n,1,1}^t. \tag{53}$$

Proof: The proof readily follows by applying the properties of amicable orthogonal designs; details are omitted due to space limitations.

Note that the effects of phase misalignment are mitigated in (51) as it depends solely on the absolute value of $g_{k,l}^{(ef)}$. In addition, (51) reveals that it is possible to mitigate such undesired effects in CF-mMIMO systems without assuming perfect detection of the code matrix. This contrasts with [1], which relies on perfect detection to demonstrate the effectiveness of DSTBC techniques in CF-mMIMO systems.

Proposition 3: The SNR of UE k can be expressed as

$$SNR_k \approx \frac{\mathbb{E}_{\mathbf{C}}\{|\mathrm{ML}_{k,n,1}^t|^2\}}{\mathbb{E}_{\mathbf{C}}\{|\mathrm{ML}_{k,n,2}^t|^2\} + \mathbb{E}_{\mathbf{C}}\{|\mathrm{ML}_{k,n,3}^t|^2\}}, \qquad (54)$$

which reduces to computing

$$SNR_k \approx \frac{\sum_{l=1}^{L} |g_{k,l}^{(ef)}|^2}{2n_s \sigma_{al}^2},$$
 (55)

where the operator $\mathbb{E}_{\mathbf{C}}$ indicates that the expectations are taken with respect to the information signals \mathbf{C}_{k}^{t} .

D. SINR Expression

The procedure for deriving the SINR closely follows the approach used for the SNR derivation. However, to accurately account for multi-user interference, the received signal block \mathbf{y}_k^t must be modeled according to (32), rather than assuming only the desired signal and noise components. Accordingly, to compute $\mathbf{Y}_{k}^{t} = (\mathbf{y}_{k}^{t})^{\mathrm{H}} \mathbf{y}_{k}^{t-1}$ in (38), \mathbf{y}_{k}^{t-1} is modeled as $\mathbf{y}_{k}^{t-1} = \sum_{l=1}^{L} \mathbf{g}_{k,l}^{(\mathrm{ef})} \left[\mathbf{C}_{k}^{t-1} \right]_{m(l,k),:} + \widetilde{\mathbf{n}}_{k}^{t-1}, \tag{56}$

$$\mathbf{y}_{k}^{t-1} = \sum_{l=1}^{L} \mathbf{g}_{k,l}^{(\text{ef})} \left[\mathbf{C}_{k}^{t-1} \right]_{m(l,k),:} + \widetilde{\mathbf{n}}_{k}^{t-1}, \tag{56}$$

where the combined effects of interference and receiver noise due to the received signal block \mathbf{y}_k^{t-1} is given by

$$\widetilde{\mathbf{n}}_{k}^{t-1} = \sum_{i=1, i \neq k}^{K} \sum_{l=1}^{L} \widetilde{\mathbf{g}}_{i,k,l}^{(\text{ef})} \left[\mathbf{C}_{i}^{t-1} \right]_{m(l,i),:} + \mathbf{n}_{k}^{t-1}.$$
 (57)

Recall that $\mathbf{DS}_k^t = \sum_{l=1}^L \mathbf{g}_{k,l}^{(\mathrm{ef})} \big[\mathbf{C}_k^t \big]_{m(l,k),:} \in \mathbb{C}^{1 \times L_k}$ denote the desired signal of UE k for the received signal block \mathbf{y}_k^t , where the last equality, i.e., $\left[\mathbf{C}_{k}^{t}\right]_{m(l,k),:} = \left[\mathbf{C}_{k}^{t-1}\right]_{m(l,k),:} \mathbf{X}_{k}^{t}$, comes from (31). Thus, we can define the received signal blocks \mathbf{y}_{k}^{t} and \mathbf{y}_{k}^{t-1} as $\mathbf{y}_{k}^{t} = \mathbf{D}\mathbf{S}_{k}^{t} + \widetilde{\mathbf{n}}_{k}^{t}$ and $\mathbf{y}_{k}^{t-1} = \mathbf{D}\mathbf{S}_{k}^{t}$ $\mathbf{DS}_k^{t-1} + \widetilde{\mathbf{n}}_k^{t-1}$, with $\widetilde{\mathbf{n}}_k^t$ being calculated in (33). Let $\mathrm{MLI}_{k,n}^t$ denote the operation $\operatorname{tr}\left\{\mathbf{A}_{n}\mathbf{Y}_{k}^{t}\right\}$ in (39). Then, we obtain

$$\mathrm{MLI}_{k,n}^t = \mathrm{MLI}_{k,n,1}^t + \mathrm{MLI}_{k,n,2}^t + \mathrm{MLI}_{k,n,3}^t + \mathrm{MLI}_{k,n,4}^t,$$
 (58) with $\mathrm{MLI}_{k,n,1}^t = \mathrm{tr} \left\{ \mathbf{A}_n (\mathbf{DS}_k^t)^H \mathbf{DS}_k^{t-1} \right\}$ representing the desired signal components and the remaining terms denoting the cross-products that are obtained as $\mathrm{MLI}_{k,n,2}^t = \mathrm{tr} \left\{ \mathbf{A}_n (\mathbf{DS}_k^t)^H \widetilde{\mathbf{n}}_k^{t-1} \right\}$, $\mathrm{MLI}_{k,n,3}^t = \mathrm{tr} \left\{ \mathbf{A}_n (\widetilde{\mathbf{n}}_k^t)^H \mathbf{DS}_k^{t-1} \right\}$, and $\mathrm{MLI}_{k,n,4}^t = \mathrm{tr} \left\{ \mathbf{A}_n (\widetilde{\mathbf{n}}_k^t)^H \widetilde{\mathbf{n}}_k^{t-1} \right\}$. Since the terms in $\mathrm{MLI}_{k,n}^t$ contain different numbers of components, the SINR is computed based on their individual power contributions.

Proposition 4: In CF-mMIMO systems employing DSTBC techniques, an expression for the DL SINR at UE k can be given in (59), and in (60) in closed form. The last term in the denominator of (60) is computed in closed form as in (61). The expressions (59)–(61) are shown on top of the next page.

IV. NUMERICAL RESULTS

We consider a CF-mMIMO network comprising L APs, each equipped with N antennas, and K single-antenna UEs. The L APs are distributed over a coverage area of $0.5 \text{ km} \times$ 0.5 km following a hard core point process (HCPP)⁶, whereas the K UEs are uniformly distributed within the same region. We focus on DL channels and assume that $\tau_c = 200$, $\tau_d = 190$, and $\tau_p = 10$. Moreover, the wrap-around technique is employed to provide a better balance regarding the amount of interference affecting each AP. The total transmission powers of UEs and APs are $p_k = 100 \,\mathrm{mW}, \; \rho_{\mathrm{max}} = 200 \,\mathrm{mW}.$ For computing the centralized power coefficients $\{\rho_k\}$, we consider the popular fractional power allocation strategy with parameters $\zeta = 0.2, \, \zeta = -0.5 \, \text{and} \, \kappa = 0.5 \, [3], \, [30].$

The SE is computed using the BER for schemes that do not admit an expression for the SE, such as DSTBC. For this purpose, the BER is calculated via Monte-Carlo simulations over different channel realizations and AP/UE locations, referred to as setups. In each setup, the received symbols are detected using the ML criterion and then mapped to bits via Gray coding. In the following, the BER is calculated for each UE over all channel realizations as [1]

$$\widetilde{SE}_k = P_f \log_2(M_o) \left(1 - \mathbb{E}_{\mathbf{h}} \left\{ BER_k \right\} \right) , \qquad (62)$$

where the value of P_f varies depending on the transmission scheme and is defined as τ_d/τ_c for conventional CF-mMIMO and $(G-1)n_s/\tau_c$ for CF-mMIMO with DSTBC. The term $\mathbb{E}_{\mathbf{h}} \left\{ \text{BER}_k \right\}$ represents the average BER across all channel realizations, and $M_o = 8$ denotes the modulation order.

The AP clustering scheme that associates the UE with the L_k AP presenting the strongest channel in its vicinity is utilized [27]. In this scheme, the UE requests a connection to the L_k APs with the greatest channel gains in its surroundings. Then, the APs accept the connection request from UE k if it has availability for a new connection, i.e., $|\mathcal{K}_l| < \tau_p$ or if the

⁶In this approach, the minimum allowed distance between any two APs is $d_{\min} = \sqrt{A/L}$, where A is the coverage area. Initially, APs are randomly placed using a homogeneous Poisson point process with density $1/d_{\min}$. APs too close to others are iteratively replaced until the distance constraint is met.

$$SINR_{k}^{(dl,3)} = \frac{\mathbb{E}_{\mathbf{C}} \{ |MLI_{k,n,1}^{t}|^{2} \}}{\sum_{z'=1}^{2} \mathbb{E}_{\mathbf{C}} \{ |MLI_{k,n,2,z'}^{t}|^{2} \} + \sum_{z'=1}^{2} \mathbb{E}_{\mathbf{C}} \{ |MLI_{k,n,3,z'}^{t}|^{2} \} + \sum_{z'=1}^{4} \mathbb{E}_{\mathbf{C}} \{ |MLI_{k,n,4,z'}^{t}|^{2} \}}$$
(59)

$$SINR_{k}^{(dl,3)} \approx \frac{\left(\sum_{l=1}^{L} |g_{k,l}^{(ef)}|^{2} / \sqrt{n_{s}}\right)^{2}}{2\left(\sigma_{dl}^{2} \sum_{l=1}^{L} |g_{k,l}^{(ef)}|^{2} + \sigma_{dl}^{2} \sum_{i=1,i\neq k}^{K} \sum_{l=1}^{L} |\widetilde{g}_{i,k,l}^{(ef)}|^{2} + \sum_{i=1,i\neq k}^{K} \sum_{l=1}^{L} \sum_{r=1}^{L} \frac{1}{L_{k}} |g_{k,l}^{(ef)}|^{2} |\widetilde{g}_{i,k,r}^{(ef)}|^{2}\right) + \mathbb{E}_{\mathbf{C}}\left\{|MLI_{k,n,4,4}^{t}|^{2}\right\}}$$
(60)

$$\mathbb{E}_{\mathbf{C}}\{|\mathrm{MLI}_{k,n,4,4}^{t}|^{2}\} \approx \sum_{\substack{i=1\\i\neq k}}^{K} \left(\sum_{l=1}^{L} \frac{\left|\widetilde{\mathbf{g}}_{i,k,l}^{(\mathrm{ef})}\right|^{4}}{n_{s}} + \sum_{l=1}^{L} \sum_{\substack{r=1\\r\neq l}}^{L} \left|\widetilde{\mathbf{g}}_{i,k,l}^{(\mathrm{ef})}\widetilde{\mathbf{g}}_{i,k,r}^{(\mathrm{ef})}\right|^{2} \left(\frac{1}{L_{k}} + \widetilde{L}_{k}\right)\right) + \sum_{\substack{i=1\\i\neq k}}^{K} \sum_{\substack{v=1\\v\neq k,v\neq i}}^{K} \sum_{l=1}^{L} \sum_{r=1}^{L} \frac{\left|\widetilde{\mathbf{g}}_{i,k,l}^{(\mathrm{ef})}\widetilde{\mathbf{g}}_{v,k,r}^{(\mathrm{ef})}\right|^{2}}{L_{k}}$$
(61)

TABLE I: Main simulation settings.

Parameter	Value
Shadow fading standard deviation, $\sigma_{\rm SF}$	4 dB
AP/UE antenna height, $h_{\rm AP}, h_{\rm UE}$	11.65 m, 1.65 m
RX noise figure (NF)	$8 \mathrm{~dB}$
Carrier frequency, bandwidth (B)	$3.5 \mathrm{GHz}, 20 \mathrm{MHz}$
Angular standard deviations (ASDs)	$\sigma_{\varphi} = \sigma_{\theta} = 15^{\circ}$
Antenna spacing	1/2 wavelength distance

channel gain from UE k exceeds that of the currently served UE with the weakest channel gain at the AP.

The 3GPP Urban Micro (UMi) path loss model is adopted for modeling the propagation channel [31]. It is considered that the shadowing terms of an AP to different UEs are correlated. Moreover, the computation of the matrices \mathbf{R}_{kl} follows the *local scattering spatial correlation model* [3]. Table I exhibits the parameters used in the UMi and \mathbf{R}_{kl} models [3], [32].

A. Impacts of Phase Misalignment in CF-mMIMO systems

Fig. 2 shows the cumulative distribution functions (CDFs) of the SE for UC CF-mMIMO systems with (Async CF) and without (Sync CF) phase misalignment effects. The phase misalignment level α is varied, and both centralized and distributed processing are evaluated using the lower and upper capacity bounds derived in (18) and (21), with each UE being served by $L_k=8$ APs.

In Figs. 2a and 2b, the SE is computed using the capacity lower bound in (21). In these ones, it can be observed that phase misalignment effects can severely degrade the SE of UC CF-mMIMO systems, particularly when $\alpha \geq \pi/8$. One can also note that the centralized processing is more susceptible to these effects, as it relies on accurate channel estimates of many UEs to suppress interference effectively. For instance, when α increases from 0 to $\pi/8$, the SE of the 95% likely UEs drops by approximately 43% and 82% for the MR and P-MMSE schemes, respectively.

The degradation in SE is also observable when it is computed using the capacity upper bound in (18). However, the impact is less pronounced as depicted in Figs. 2c and 2d. This is because the SINR in (18) is derived from (15), where the expectation is taken after the squared magnitude operation, which is analogous to multiplying a term by its complex conjugate. This procedure is similar to that performed by DSTBC schemes in (38), which generates better resilience to the effects of phase misalignment. This robustness can

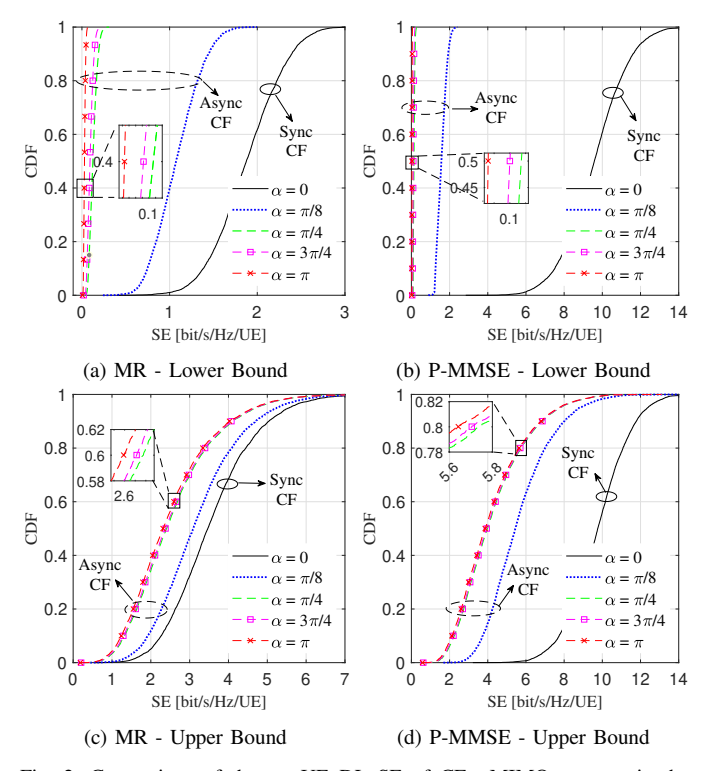


Fig. 2: Comparison of the per-UE DL SE of CF-mMIMO systems in the presence of phase misalignment effects by varying the value of α in (18) and (21) from 0 to π . Eqs. (18) and (21) refer to the upper and lower bounds, respectively. Parameters settings: $L=40,\,K=20,\,N=4$ and $L_k=8$.

be further understood by analyzing the numerator of (18), where the term $(1-\tilde{\nu})\sum_{l=1}^L \left|\mathbf{h}_{k,l}^{(\mathrm{ef})}\right|^2$ remains significant even when $\alpha=\pi$ increases, since $\tilde{\nu}=\mathrm{sinc}^2(\alpha)$. In contrast, the numerator of (21), given by $\tilde{\nu}\left|\sum_{l=1}^L \mathbb{E}_{\mathbf{h}}\left\{\mathbf{h}_{k,l}^{(\mathrm{ef})}\right\}\right|^2$, directly scales with $\tilde{\nu}$ and thus decreases as α increases. On the other hand, it is important to note that (18) is derived under idealized assumptions, such as the UE having access to the perfect CSI. In other words, although it exhibits reduced susceptibility to phase misalignment effects, this benefit relies on assumptions that may not hold in practical scenarios.

B. Performance of DSTBC schemes in CF-mMIMO

Fig. 3 compares the SE achieved by the proposed solution with that of conventional UC CF-mMIMO systems. To this end, each UE is served by $L_k=2$ APs, and the SE is computed according to (62). One can note that the proposed approach outperforms UC CF-mMIMO systems affected

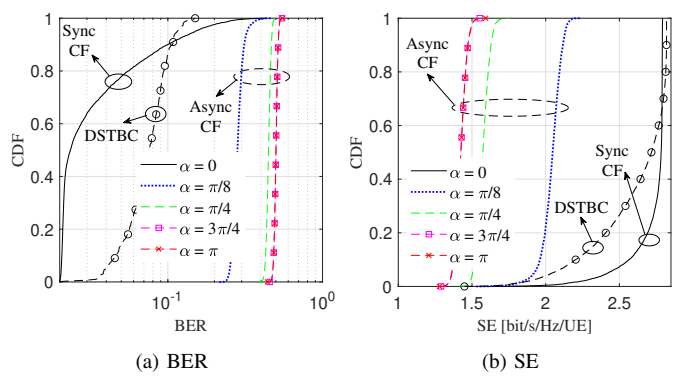


Fig. 3: CDF of (a) BER (b) per-UE SE for conventional and DSTBC-based CF-mMIMO systems under varying phase misalignment levels. Parameters: $L=100,\ K=20,\ L_k=2,\ N=4.$ Precoding scheme: P-MMSE.

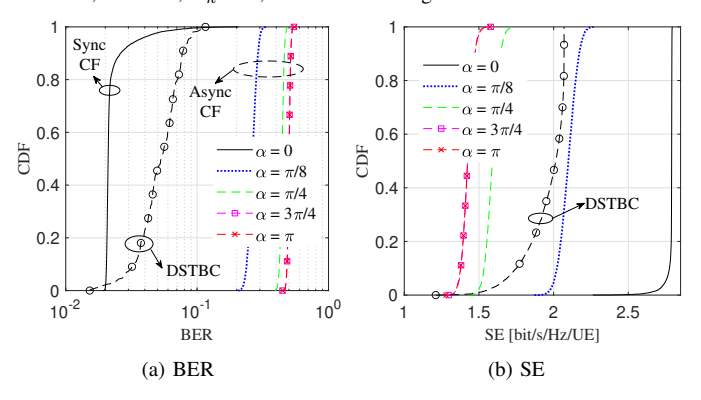


Fig. 4: CDF of (a) BER (b) per-UE SE for conventional and DSTBC-based CF-mMIMO systems under varying phase misalignment levels. Parameters: $L=100,\ K=20,\ L_k=4,\ N=4.$ Precoding scheme: P-MMSE.

by phase misalignment and approaches the performance of perfectly synchronized systems. The proposed approach can even perform slightly better than synchronized CF-mMIMO systems (from the 65% likely UEs), as the product in (38) tends to reinforce the desired signal. Therefore, this effect becomes particularly evident when UEs experience strong channels and low levels of interference.

However, the gains afforded by the proposed solution tend to decrease for $L_k > 2$, as illustrated in Fig. 4. It is possible to observe that asynchronous UC CF-mMIMO systems can outperform DSTBC-based systems when $\alpha \leq \pi/8$, mainly due to the negative impact of the code rate in DSTBC schemes. For instance, when $L_k = 4$, the code rate equals 3/4, thereby reducing the SE achieved by the proposed approach by 25%. In other words, although DSTBC schemes offer a feasible approach to mitigate phase misalignment in CF-mMIMO systems, the code rate remains a limiting factor in these schemes, particularly for $L_k \geq 4$. On the other hand, the gains provided by the proposed approach are evident for $L_k = 2$ and remain consistent even for higher modulation orders, as depicted in Fig. 5. Moreover, the proposed approach also presents improvements in terms of BER in Fig. 4.

C. SINR analysis

To provide a more detailed performance evaluation of the proposed DSTBC-based system, Fig. 6 presents results based on the derived SINR expression, supported by BER simulations. As expected, the SINR slightly increases with the

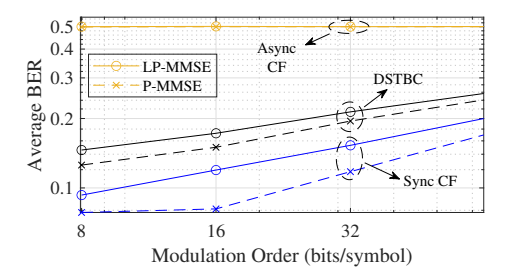


Fig. 5: Average BER versus the modulation order. Parameters setting: L=40, K=20, $L_k=2$, N=4, and $\alpha=\pi$. Precoding scheme: P-MMSE.

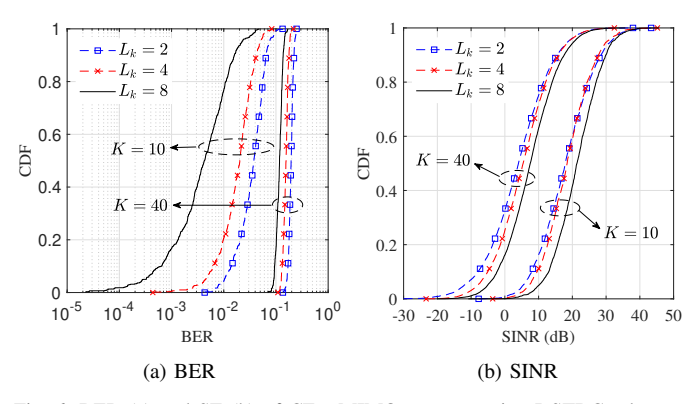


Fig. 6: BER (a) and SE (b) of CF-mMIMO systems using DSTBC schemes by varying the number of APs serving the UE, i.e., L_k . Parameters setting: $L=40,\ K=20,$ and N=4. Precoding scheme: LP-MMSE.

number of APs L_k serving the UE, but the gains are modest. This is because the product $(\mathbf{y}_k^t)^H \mathbf{y}_k^{t-1}$ in (38) can amplify not only the desired signal but also the interference as more APs serve the UE, as observed in (60). The same observation can be made with respect to the BER as depicted in Fig. 6a.

It is worth noting that we include both the SINR and BER results in Fig. 6 because the BER provides practical insights into error performance and helps validate the analytical SINR. However, BER evaluation can be computationally intensive and depends on the modulation scheme. In contrast, the derived SINR enables a more general and efficient performance assessment of CF-mMIMO systems using DSTBC schemes.

V. Conclusions

This paper investigated DSTBC techniques as a robust solution for phase misalignments in UC CF-mMIMO systems. We first quantified the performance degradation in conventional systems by deriving capacity bounds and a closed-form SE for MR precoding under random phase misalignments. This analysis, covering both centralized and distributed processing, confirmed that misalignments severely degrade SE, especially in centralized systems, unless the errors are negligible or perfect CSI is available.

We then derived SNR and SINR expressions for the proposed DSTBC scheme. Our results demonstrate that DSTBC effectively restores performance, approaching the SE and BER of a perfectly synchronized system without requiring perfect CSI. While the inherent DSTBC code rate can limit the peak SE when many APs serve a UE, the approach consistently provides significant BER gains. Future work can extend this analysis to include fronthaul limitations and mobility.

APPENDIX

A. Proof of Proposition 3

In order to compute the SNR in (55), we need to compute $\mathbb{E}_{\mathbf{C}}\{|\mathrm{ML}_{k,n,2}^t|^2\}$ and $\mathbb{E}_{\mathbf{C}}\{|\mathrm{ML}_{k,n,3}^t|^2\}$.

1) Compute $\mathbb{E}_{\mathbf{C}}\{|\mathrm{ML}_{k,n,2}^t|^2\}$: By applying the cyclic property of the trace in (43), let us rewrite $\mathrm{ML}_{k,n,2}^t$ as

$$ML_{k,n,2}^{t} = \sum_{l=1}^{L} \left[\mathbf{C}_{k}^{t-1} \right]_{m(l,k),:} \mathbf{g}_{k,l}^{(ef)} \mathbf{A}_{n} \left(\mathbf{n}_{k}^{t} \right)^{H}.$$
 (63)

Hence, the term $|\mathrm{ML}_{k,n,2}^t|^2 = \mathrm{ML}_{k,n,2}^t (\mathrm{ML}_{k,n,2}^t)^{\mathrm{H}}$ becomes

$$\sum_{l=1}^{L} \sum_{l'=1}^{L} \left[\mathbf{C}_{k}^{t-1} \right]_{m'(l',k),:} \mathbf{F}_{k,l,l',n}^{t} \left[\mathbf{C}_{k}^{t-1} \right]_{m(l,k),:}^{\mathbf{H}}, \quad (64)$$

with $\mathbf{F}_{k,l,l',n}^t = \left(\mathbf{g}_{k,l}^{(\mathrm{ef})}\right)^{\mathrm{H}} \mathbf{g}_{k,l'}^{(\mathrm{ef})} \mathbf{A}_n \left(\mathbf{n}_k^t\right)^{\mathrm{H}} \mathbf{n}_k^t \mathbf{A}_n^{\mathrm{H}}$. Given that $\left|\mathrm{ML}_{k,n,2}^t\right|^2$ is a scalar, it can also be written as

$$|\mathrm{ML}_{k,n,2}^t|^2 = \sum_{l=1}^L \sum_{l'=1}^L \mathrm{tr} \{ (\mathbf{C}_{k,m,m',l,l'}^{t-1,t-1})^{\mathrm{H}} \mathbf{F}_{k,l,l',n}^t \},$$
 (65)

where $\mathbf{C}_{k,m,m',l,l'}^{t-1,t-1} = \left[\mathbf{C}_k^{t-1}\right]_{m(l,k),:}^{\mathbf{H}} \left[\mathbf{C}_k^{t-1}\right]_{m'(l',k),:}^{\mathbf{H}}$. Since matrices $\mathbf{C}_{k,m,m',l,l'}^{t-1,t-1}$ and $\mathbf{F}_{k,l,l',n}^{t}$ are statistically independent, $\mathbb{E}_{\mathbf{C}}\left\{\left|\mathbf{ML}_{k,n,2}^{t}\right|^{2}\right\}$ is obtained as

$$\sum_{l=1}^{L} \sum_{l'=1}^{L} \operatorname{tr} \left\{ \mathbb{E}_{\mathbf{C}} \left\{ \mathbf{C}_{k,m,m',l,l'}^{t-1,t-1} \right\} \mathbb{E}_{\mathbf{C}} \left\{ \mathbf{F}_{k,l,l',n}^{t} \right\} \right\}.$$
 (66)

Provided that $\mathbf{A}_n \mathbf{A}_n^{\mathrm{H}} = \mathbf{I}_{L_k}$, the term $\mathbb{E}_{\mathbf{C}} \left\{ \mathbf{F}_{k,l,l',n}^t \right\}$ is given by $\mathbb{E}_{\mathbf{C}} \left\{ \mathbf{F}_{k,l,l',n}^t \right\} = \left(\mathbf{g}_{k,l}^{(\mathrm{ef})} \right)^{\mathrm{H}} \mathbf{g}_{k,l'}^{(\mathrm{ef})} \sigma_{\mathrm{dl}}^2 \mathbf{I}_{L_k}$. Then, by computing $\mathrm{tr} \left\{ \mathbf{C}_{k,m,m',l,l'}^{t-1,t-1} \right\}$ in (50), we have

$$\mathbb{E}_{\mathbf{C}}\{|\mathrm{ML}_{k,n,2}^{t}|^{2}\} = \sigma_{\mathrm{dl}}^{2} \sum_{l=1}^{L} |\mathbf{g}_{k,l}^{(\mathrm{ef})}|^{2}.$$
 (67)

2) Compute $\mathbb{E}_{\mathbf{C}}\{|\mathrm{ML}_{k,n,3}^t|^2\}$: Let us rewrite $\mathrm{ML}_{k,n,3}^t$ in (44) as $\mathrm{ML}_{k,n,3}^t = \sum_{l=1}^L \mathbf{g}_{k,l}^{(\mathrm{ef})\,\mathrm{H}}\mathbf{n}_k^{t-1}\mathbf{A}_n \big[\mathbf{C}_k^t\big]_{m(l,k),:}^\mathrm{H}$, with $\big[\mathbf{C}_k^t\big]_{m(l,k),:}^t = \big[\mathbf{C}_k^{t-1}\big]_{m(l,k),:}\mathbf{X}_k^t$. Thus,

$$|\mathrm{ML}_{k,n,3}^{t}|^{2} = \sum_{l=1}^{L} \sum_{l'=1}^{L} \mathrm{tr} \left\{ \left(\mathbf{C}_{k,m,m',l,l'}^{t,t} \right)^{\mathrm{H}} \mathbf{F}_{k,m,m',l,l',n}^{t-1} \right\}, (68)$$

where $\mathbf{C}_{k,m,m',l,l'}^{t,t}=\left[\mathbf{C}_k^t\right]_{m(l,k),:}^{\mathbf{H}}\left[\mathbf{C}_k^t\right]_{m'(l',k),:}^{\mathbf{H}}$. Hence,

$$\mathbb{E}_{\mathbf{C}}\{|\mathrm{ML}_{k,n,3}^{t}|^{2}\} = \sigma_{\mathrm{dl}}^{2} \sum_{l=1}^{L} |\mathbf{g}_{k,l}^{(\mathrm{ef})}|^{2}. \tag{69}$$

B. Proof of Proposition 4

To compute the SINR in (60), it is necessary to evaluate the power of each component in the denominator of (59).

1) Compute $\mathbb{E}_{\mathbf{C}}\{|\mathrm{MLI}_{k,n,2,1}^t|^2\}$ and $\mathbb{E}_{\mathbf{C}}\{|\mathrm{MLI}_{k,n,2,2}^t|^2\}$: Let the term $\mathrm{MLI}_{k,n,2}^t = \mathrm{tr}\{\mathbf{A}_n(\mathbf{DS}_k^t)^H\widetilde{\mathbf{n}}_k^{t-1}\}$ be rewritten as $\mathrm{MLI}_{k,n,2}^t = \mathrm{MLI}_{k,n,2,1}^t + \mathrm{MLI}_{k,n,2,2}^t$, with

$$\mathbf{MLI}_{k,n,2,1}^{t} = \sum_{i=1,i\neq k}^{K} \sum_{l=1}^{L} \sum_{r=1}^{L} \operatorname{tr} \left\{ \mathbf{g}_{k,l}^{(\text{ef})} \mathbf{H} \widetilde{\mathbf{g}}_{i,k,r}^{(\text{ef})} \mathbf{A}_{n} \mathbf{C}_{k,i,m,\mu,l,r}^{t,t-1} \right\},$$

where $\mathbf{C}_{k,i,m,\mu,l,r}^{t,t-1} = \left[\mathbf{C}_{k}^{t}\right]_{m(l,k),:}^{\mathbf{H}} \left[\mathbf{C}_{i}^{t-1}\right]_{\mu(r,i),:}^{}$. In addition, $\left[\mathbf{C}_{k}^{t}\right]_{m(l,k),:} = \left[\mathbf{C}_{k}^{t-1}\right]_{m(l,k),:}^{} \mathbf{X}_{k}^{t}$ and $\mathbf{MLI}_{k,n,2,2}^{t}$ is calculated as $\mathbf{MLI}_{k,n,2,2}^{t} = \mathrm{tr}\left\{\sum_{l=1}^{L}\mathbf{g}_{k,l}^{(\mathrm{ef})\mathbf{H}}\mathbf{A}_{n}\left[\mathbf{C}_{k}^{t}\right]_{m(l,k),:}^{\mathbf{H}}\mathbf{n}_{k}^{t-1}\right\}$. By noting that $\mathbf{MLI}_{k,n,2,2}^{t}$ corresponds to $\mathbf{ML}_{k,n,3}^{t}$ in (44), $\mathbb{E}_{\mathbf{C}}\{|\mathbf{MLI}_{k,n,2,2}^{t}|^{2}\}$ can be calculated as

$$\mathbb{E}_{\mathbf{C}}\{|\mathrm{MLI}_{k,n,2,2}^{t}|^{2}\} = \sigma_{\mathrm{dl}}^{2} \sum_{l=1}^{L} |\mathbf{g}_{k,l}^{(\mathrm{ef})}|^{2}. \tag{71}$$

For computing $\mathbb{E}_{\mathbf{C}}\{|\mathrm{MLI}_{k,n,2,1}^t|^2\}$, the trace in (70) can be rewritten as $\mathbf{g}_{k,l}^{(\mathrm{ef})}\mathbf{H}\widetilde{\mathbf{g}}_{i,k,r}^{(\mathrm{ef})}[\mathbf{C}_i^{t-1}]_{\mu(r,i),:}\mathbf{A}_n[\mathbf{C}_k^t]_{m(l,k),:}^{\mathrm{H}}$. Hence, $|\mathrm{MLI}_{k,n,2,1}^t|^2$ is given by

$$\sum_{\substack{i=1\\i\neq k}}^{K} \sum_{\substack{i'=1\\i'\neq k}}^{K} \sum_{l=1}^{L} \sum_{l'=1}^{L} \sum_{r=1}^{L} \sum_{r'=1}^{L} U_{k,i,i',m,m',\mu,\mu',l,l',r,r',n}^{t},$$
 (72)

where $U^t_{k,i,i',m,m',\mu,\mu',l,l',r,r',n}$ is obtained as

$$\operatorname{tr}\left\{\mathbf{g}_{k,i,i',l,l',r,r'}\mathbf{C}_{i,i',\mu,\mu',r,r'}^{t-1,t-1}\mathbf{A}_{n}\mathbf{C}_{k,m,m',l,l'}^{t,t}\mathbf{A}_{n}^{\mathrm{H}}\right\},\tag{73}$$

with $\mathbf{g}_{k,i,i',l,l',r,r'} = \mathbf{g}_{k,l}^{(\mathrm{ef})\mathrm{H}} \mathbf{g}_{k,l'}^{(\mathrm{ef})} \widetilde{\mathbf{g}}_{i',k,r'}^{(\mathrm{ef})\mathrm{H}} \widetilde{\mathbf{g}}_{i,k,r}^{(\mathrm{ef})}$, and the matrix $\mathbf{C}_{i,i',\mu,\mu',r,r'}^{t-1,t-1}$ being calculated as

$$\mathbf{C}_{i,i',\mu,\mu',r,r'}^{t-1,t-1} = \left[\mathbf{C}_{i'}^{t-1}\right]_{\mu'(r',i'),:}^{\mathbf{H}} \left[\mathbf{C}_{i}^{t-1}\right]_{\mu(r,i),:}^{\mathbf{H}}.$$
 (74)

Besides, $\mathbf{C}_{k,m,m',l,l'}^{t,t} = \left[\mathbf{C}_k^t\right]_{m(l,k),:}^{\mathbf{H}} \left[\mathbf{C}_k^t\right]_{m'(l',k),:}^{\mathbf{H}}$. Hence, one can evaluate $\mathbb{E}_{\mathbf{C}}\left\{U_{k,i,i',m,m',\mu,\mu',l,l',r,r',n}^t\right\}$ as

$$\operatorname{tr}\left\{g_{k,i,i',l,l',r,r'}\mathbb{E}_{\mathbf{C}}\left\{\mathbf{C}_{i,i',\mu,\mu',r,r'}^{t-1,t-1}\mathbf{A}_{n}\mathbf{C}_{k,m,m',l,l'}^{t,t}\mathbf{A}_{n}^{\mathbf{H}}\right\}\right\}. (75)$$

Given that the information signals of UEs i,i' and k are independent, the expected values of $\mathbf{C}_{i,i',\mu,\mu',r,r'}^{t-1,t-1}$ and $\mathbf{C}_{k,m,m',l,l'}^{t,t}$ can be obtained separately. Moreover, $\mathbb{E}_{\mathbf{C}} \left\{ \mathbf{C}_{i,i',\mu,\mu',r,r'}^{t-1,t-1} \right\} = \mathbf{0}$ for $i \neq i'$, as the information signals of different UEs are statistically uncorrelated. One can also note that since the information signals generated in (30) are composed of zeromean complex data symbols drawn from a unitary constellation, the following property holds

$$\mathbb{E}_{\mathbf{C}} \left\{ \mathbf{C}_{k,m,m',l,l'}^{t,t} \right\} = \begin{cases} \frac{1}{L_k} \mathbf{I}_{L_k} & \text{if } m(l,k) = m'(l',k), \\ \mathbf{0} & \text{if } m(l,k) \neq m'(l',k). \end{cases}$$
(76)

Similarly, it holds that $\mathbb{E}_{\mathbf{C}}\left\{\mathbf{C}_{i,i',\mu,\mu',r,r'}^{t-1,t-1}\right\} = (1/L_k)\mathbf{I}_{L_k}$ for $\mu(r,i) = \mu'(r',i')$, and equals $\mathbf{0}$ otherwise. Thus,

$$\mathbb{E}_{\mathbf{C}}\{|\mathrm{MLI}_{k,n,2,1}^{t}|^{2}\} = \sum_{\substack{i=1\\i\neq k}}^{K} \sum_{l=1}^{L} \sum_{r=1}^{L} \frac{1}{L_{k}} |\mathbf{g}_{k,l}^{(\mathrm{ef})}|^{2} |\widetilde{\mathbf{g}}_{i,k,r}^{(\mathrm{ef})}|^{2}. \quad (77)$$

2) Compute $\mathbb{E}_{\mathbf{C}}\{|\mathrm{MLI}_{k,n,3,1}^t|^2\}$ and $\mathbb{E}_{\mathbf{C}}\{|\mathrm{MLI}_{k,n,3,2}^t|^2\}$: Let us define $\mathrm{MLI}_{k,n,3}^t-\mathrm{tr}\{\mathbf{A}_n(\widetilde{\mathbf{n}}_k^t)^H\mathbf{DS}_k^{t-1}\}$ as $\mathrm{MLI}_{k,n,3}^t=\mathrm{MLI}_{k,n,3,1}^t+\mathrm{MLI}_{k,n,3,2}^t$, with $\mathrm{MLI}_{k,n,3,1}^t$ being found as

$$\sum_{i=1}^{K} \sum_{j=1}^{L} \sum_{k=1}^{L} \operatorname{tr} \left\{ \widetilde{\mathbf{g}}_{i,k,r}^{(\text{ef})H} \mathbf{g}_{k,l}^{(\text{ef})} \mathbf{A}_{n} \mathbf{C}_{i,k,m,\mu,l,r}^{t,t-1} \right\}.$$
 (78)

In (78), we have $\mathbf{C}_{i,k,m,\mu,l,r}^{t,t-1} = \left[\mathbf{C}_i^t\right]_{\mu(r,i),:}^{\mathbf{H}} \left[\mathbf{C}_k^{t-1}\right]_{m(l,k),:}^{}$, and the term $\mathrm{MLI}_{k,n,3,2}^t$ is calculated as $\mathrm{MLI}_{k,n,3,2}^t = \mathrm{tr}\left\{\sum_{l=1}^L \mathbf{g}_{k,l}^{(\mathrm{ef})} \mathbf{A}_n \left(\mathbf{n}_k^t\right)^{\mathbf{H}} \left[\mathbf{C}_k^{t-1}\right]_{m(l,k),:}^{}\right\}$. Moreover, note that $\mathrm{MLI}_{k,n,3,2}^t$ corresponds to $\mathrm{ML}_{k,n,2}^t$ in (43). Therefore, $\mathbb{E}_{\mathbf{C}}\left\{|\mathrm{MLI}_{k,n,3,2}^t|^2\right\}$ is obtained as follows

$$\mathbb{E}_{\mathbf{C}}\{|\mathrm{MLI}_{k,n,3,2}^{t}|^{2}\} = \sigma_{\mathrm{dl}}^{2} \sum_{l=1}^{L} |\mathbf{g}_{k,l}^{(\mathrm{ef})}|^{2}. \tag{79}$$

The computation of $\mathbb{E}_{\mathbf{C}}\{|\mathrm{MLI}_{k,n,3,1}^t|^2\}$ can be derived analogously to $\mathbb{E}_{\mathbf{C}}\{|\mathrm{MLI}_{k,n,2,1}^t|^2\}$ given that $\mathrm{MLI}_{k,n,3,1}^t$ and $\mathrm{MLI}_{k,n,2,1}^t$ share the same structure, as indicated in (78) and (70). Consequently, we have

$$\mathbb{E}_{\mathbf{C}}\{|\mathrm{MLI}_{k,n,3,1}^{t}|^{2}\} = \sum_{\substack{i=1\\i\neq k}}^{K} \sum_{l=1}^{L} \sum_{r=1}^{L} \frac{1}{L_{k}} |\mathbf{g}_{k,l}^{(\mathrm{ef})}|^{2} |\widetilde{\mathbf{g}}_{i,k,r}^{(\mathrm{ef})}|^{2}. \quad (80)$$

3) Computing $\sum_{z'=1}^4 \mathbb{E}_{\mathbf{C}}\{|\mathrm{MLI}_{k,n,4,z'}^t|^2\}$: Let the interference signals at UE k during the received blocks \mathbf{y}_k^t and \mathbf{y}_k^{t-1} be defined as $\mathbf{IS}_k^t = \sum_{i=1,i\neq k}^K \sum_{l=1}^L \widetilde{\mathbf{g}}_{i,k,l}^{(\mathrm{ef})} [\mathbf{C}_i^{t-1}]_{m(l,i),:} \mathbf{X}_i^t$ and $\mathbf{IS}_k^{t-1} = \sum_{i=1,i\neq k}^K \sum_{l=1}^L \widetilde{\mathbf{g}}_{i,k,l}^{(\mathrm{ef})} [\mathbf{C}_i^{t-1}]_{m(l,i),:}$. Hence, the combined effects of noise and interference can be rewritten as $\widetilde{\mathbf{n}}_k^t = \mathbf{IS}_k^t + \mathbf{n}_k^t$ and $\widetilde{\mathbf{n}}_k^{t-1} = \mathbf{IS}_k^{t-1} + \mathbf{n}_k^{t-1}$. Since the last term of (58) is defined as $\mathrm{MLI}_{k,n,4}^t - \mathrm{tr}\{\mathbf{A}_n(\widetilde{\mathbf{n}}_k^t)^H \widetilde{\mathbf{n}}_k^{t-1}\}$, we have

$$\text{MLI}_{k,n,4}^t = \sum_{z'=1}^4 \text{MLI}_{k,n,4,z'}^t$$
, (81)

where the first term $\mathrm{MLI}_{k,n,4,1}^t = \mathbf{A}_n(\mathbf{n}_k^t)^{\mathrm{H}}\mathbf{n}_k^{t-1}$ can be neglected if the noise variance is small enough. The second term is defined as $\mathrm{MLI}_{k,n,4,2}^t = \mathbf{A}_n(\mathbf{n}_k^t)^{\mathrm{H}}\mathbf{IS}_k^t$, i.e.,

$$\sum_{i=1,i\neq k}^{K} \sum_{l=1}^{L} \operatorname{tr}\left\{\widetilde{\mathbf{g}}_{i,k,l}^{(\mathrm{ef})} \mathbf{A}_{n} \left(\mathbf{n}_{k}^{t}\right)^{\mathrm{H}} \left[\mathbf{C}_{i}^{t-1}\right]_{m(l,i),:}\right\}. \quad (82)$$

Then, by using the cyclic property of the trace and following the same procedure we utilized to derive (72) and (73). The term $|\text{MLI}_{k,n,4,2}^t|^2$ can be written as

$$|\mathrm{MLI}_{k,n,4,2}^{t}|^{2} = \sum_{\substack{i=1\\i\neq k}}^{K} \sum_{\substack{i'=1\\i'\neq k}}^{K} \sum_{l=1}^{L} \sum_{l'=1}^{L} \widetilde{U}_{i,i',k,m,m',l,l',n}^{t}, \qquad (83)$$

with $\widetilde{U}_{i,i',k,m,m',l,l',n}^t$ being given by

$$\operatorname{tr}\left\{\widetilde{\mathbf{g}}_{i',i,k,l',l}\widetilde{\mathbf{C}}_{i',i,k,m',m,l',l}^{t-1,t-1}\mathbf{A}_{n}(\mathbf{n}_{k}^{t})^{\mathrm{H}}\mathbf{n}_{k}^{t}\mathbf{A}_{n}^{\mathrm{H}}\right\},\tag{84}$$

where $\widetilde{\mathbf{C}}_{i',i,k,m',m,l',l}^{t-1,t-1} = \left[\mathbf{C}_{i'}^{t-1}\right]_{m'(l',i'),:}^{\mathbf{H}} \left[\mathbf{C}_{i}^{t-1}\right]_{m(l,i),:}^{\mathbf{H}}$ and $\widetilde{\mathbf{g}}_{i',i,k,l',l} = \widetilde{\mathbf{g}}_{i',k,l'}^{(\mathrm{ef})}\widetilde{\mathbf{g}}_{i,k,l}^{(\mathrm{ef})}$ which results in

$$\mathbb{E}_{\mathbf{C}}\{|\text{MLI}_{k,n,4,2}^{t}|^{2}\} = \sigma_{\text{dl}}^{2} \sum_{i=1, i \neq k}^{K} \sum_{l=1}^{L} \left|\widetilde{\mathbf{g}}_{i,k,l}^{(\text{ef})}\right|^{2}. \quad (85)$$

The computation of $\mathbb{E}_{\mathbf{C}}\{|\mathrm{MLI}_{k,n,4,3}^t|^2\}$ follows a similar procedure to that used to obtain $\mathbb{E}_{\mathbf{C}}\{|\mathrm{MLI}_{k,n,4,2}^t|^2\}$, since both have a similar structure. That is, $\mathrm{MLI}_{k,n,4,3}^t$ is defined as $\mathrm{MLI}_{k,n,4,3}^t = \mathbf{A}_n \big(\mathbf{IS}_k^t\big)^{\mathrm{H}} \mathbf{n}_k^{t-1}$. Thus,

$$\mathrm{MLI}_{k,n,4,3}^{t} = \sum_{\substack{i=1\\i\neq k}}^{K} \sum_{l=1}^{L} \mathrm{tr}\left\{ \left(\widetilde{\mathbf{g}}_{i,k,l}^{(\mathrm{ef})}\right)^{\mathrm{H}} \mathbf{A}_{n} \left[\mathbf{C}_{i}^{t}\right]_{m(l,i),:}^{\mathrm{H}} \mathbf{n}_{k}^{t-1} \right\}. \tag{86}$$

Consequently,

$$\mathbb{E}_{\mathbf{C}}\{|\mathrm{MLI}_{k,n,4,3}^{t}|^{2}\} = \sigma_{\mathrm{dl}}^{2} \sum_{i=1, i \neq k}^{K} \sum_{l=1}^{L} |\widetilde{\mathbf{g}}_{i,k,l}^{(\mathrm{ef})}|^{2}. \quad (87)$$

The calculations related to the last term of (81) involve several summations, since $\mathrm{MLI}_{k,n,4,4}^t = \mathbf{A}_n \big(\mathbf{IS}_k^t\big)^H \mathbf{IS}_k^{t-1}$. Therefore, from this point onward, we will adopt a compact notation for multiple summations to enhance brevity: a single summation operator applied to multiple indices should be understood as representing multiple summations, one for each distinct index involved. Let $\mathcal{K} = \{1, \dots, K\}$ denote the indices of all UEs in the network. By doing so, $\mathrm{MLI}_{k,n,4,4}^t$ can be defined as

work. By doing so,
$$\mathrm{MLI}_{k,n,4,4}^c$$
 can be defined as
$$\sum_{\substack{1 \leq i \leq K \\ 1 \leq v \leq K \\ \{i,v\} \subset \mathcal{K} \setminus \{k\}}} \sum_{\substack{1 \leq l \leq L \\ 1 \leq r \leq L}} \overline{\mathbf{g}}_{i,v,k,l,r}^{(\mathrm{ef})} \overline{\mathbf{C}}_{v,i,k,\mu,m,r,l,n}^{t-1,t}, \tag{88}$$

with $\bar{\mathbf{g}}_{i,v,k,l,r}^{(\mathrm{ef})} = (\tilde{\mathbf{g}}_{i,k,l}^{(\mathrm{ef})})^{\mathrm{H}} \tilde{\mathbf{g}}_{v,k,r}^{(\mathrm{ef})}$ and $\bar{\mathbf{C}}_{v,i,k,\mu,m,r,l,n}^{t-1,t}$ being calculated as $\bar{\mathbf{C}}_{v,i,k,\mu,m,r,l,n}^{t-1,t} = \left[\mathbf{C}_v^{t-1}\right]_{\mu(r,v),:} \mathbf{A}_n \left[\mathbf{C}_i^t\right]_{m(l,i),:}^{\mathrm{H}}$. After defining (88), $|\mathrm{MLI}_{k,n,4,4}^t|^2$ can be expressed as

$$\sum_{\substack{1 \le i \le K \\ 1 \le i' \le K \\ 1 \le v \le K \\ 1 \le v' \le K \\ 1 \le v' \le K \\ 1 \le i' \le L \\ 1 \le v' \le K \\ 1 \le r' \le L \\ 1 \le L \\ 1 \le r' \le L \\ 1 \le L$$

where $\overline{U}_{i,i',v,v',k,m,m',\mu,\mu',l,l',r,r',n}^t$ is defined as

$$\operatorname{tr}\left\{\bar{\mathbf{g}}_{i,i',v,v',k,l,l',r,r'}\mathbf{C}_{v',v,\mu',\mu,r',r}^{t-1,t-1}\widetilde{\mathbf{C}}_{i,i',m,m',l,l',n}^{t,t},\right\},\quad(90)$$

where $\bar{\mathbf{g}}_{i,i',v,v',k,l,l',r,r'} = (\tilde{\mathbf{g}}_{i,k,l}^{(\mathrm{ef})})^{\mathrm{H}} \tilde{\mathbf{g}}_{i',k,l'}^{(\mathrm{ef})} (\tilde{\mathbf{g}}_{v',k,r'}^{(\mathrm{ef})})^{\mathrm{H}} \tilde{\mathbf{g}}_{v,k,r}^{(\mathrm{ef})}$ and $\mathbf{C}_{v',v,\mu',\mu,r',r}^{t-1,t-1}$ is given by

$$\mathbf{C}_{v',v,\mu',\mu,r',r}^{t-1,t-1} = \left[\mathbf{C}_{v'}^{t-1}\right]_{\mu'(r',v'),:}^{\mathbf{H}} \left[\mathbf{C}_{v}^{t-1}\right]_{\mu(r,v),:}^{\mathbf{H}}. \tag{91}$$

The term $\widetilde{\mathbf{C}}_{i,i',m,m',l,l',n}^{t,t}$ is obtained as

$$\widetilde{\mathbf{C}}_{i,i',m,m',l,l',n}^{t,t} = \mathbf{A}_n \left[\mathbf{C}_{i}^{t} \right]_{m(l,i)::}^{\mathbf{H}} \left[\mathbf{C}_{i'}^{t} \right]_{m'(l',i')::}^{\mathbf{A}} \mathbf{A}_n^{\mathbf{H}}. \tag{92}$$

One can note that computing $\mathbb{E}_{\mathbf{C}}\{|\mathrm{MLI}_{k,n,4,4}^t|^2\}$ is not trivial, since it involves several cross-products and summations. Thus, we break the calculation of $\mathbb{E}_{\mathbf{C}}\{|\mathrm{MLI}_{k,n,4,4}^t|^2\}$ into five cases, each corresponding to a different combination of UE indices in (89). In the first case, we compute $\mathbb{E}_{\mathbf{C}}\{|\mathrm{MLI}_{k,n,4,4}^t|^2\}$ assuming an entirely different set of UEs, i.e., all indices v, v', i, and i' are distinct. In the second case, we consider a scenario with only one distinct UE, e.g., $i \neq i'$, with i' = v = v'. In these two cases, $\mathbb{E}_{\mathbf{C}}\{|\mathrm{MLI}_{k,n,4,4}^t|^2\}$ is approximately zero as the information signals transmitted by different UEs are composed of zero-mean complex-valued symbols. The same notion applies when $v \neq v'$ and $i \neq i'$. Consequently, only the fourth and fifth cases remain. In the fourth case, we have i = i' = v = v', while in the fifth case, i = i' and v = v', with $i \neq v$. Therefore, for the sole purpose of computing $\mathbb{E}_{\mathbf{C}}\{|\mathrm{MLI}_{k,n,4,4}^t|^2\}$, equation (89) can be rewritten as

$$\sum_{\substack{1 \leq i \leq K \\ 1 \leq v \leq K \\ \{i,v\} \subset \mathcal{K} \setminus \{k\}}} \sum_{\substack{1 \leq l \leq L \\ 1 \leq l' \leq L \\ 1 \leq r \leq L \\ 1 \leq r' \leq L}} \overline{U}_{i,v,k,m,m',\mu,\mu',l,l',r,r',n}^{t}. \tag{93}$$

The above expression can be further simplified by analyzing the indices of the information signal rows, such as m(l,i) and $\mu'(r',v')$. To perform this simplification, the following results were obtained numerically through Monte-Carlo simulations. The results reveal that for two distinct UEs (i.e., $i \neq v$), the expected value in (93) is non-zero only in two specific scenarios: 1) when m(l,i) = m'(l',i') and $\mu(r,v) = \mu'(r',v')$, with $m(l,i) \neq \mu(r,v)$; and 2) when all row indices are equal, i.e., $m(l,i) = m'(l',i') = \mu(r,v) = \mu'(r',v')$. Similarly, when i = v, the same reasoning holds. Nonetheless, an additional case must be considered, which yields a non-zero contribution when $\mu(r,v) = m(l,i)$ and $\mu'(r',v') = m'(l',i')$. Based on the above discussion, (93) simplifies to

$$\sum_{\substack{1 \le l \le L \\ 1 \le \mu \le L}} \sum_{\substack{1 \le i \le K \\ 1 \le \nu \le K \\ \{i, v\} \subset \overline{K} \setminus \{k\}}} \mathbb{E}_{\mathbf{C}} \{ \overline{U}_{i, \nu, k, \mu, m, l, r, n}^t \} + \sum_{\substack{1 \le i \le K \\ i \ne k}} \mathbb{E}_{\mathbf{C}} \{ \widetilde{U}_{i, k, \mu, m, l, r, n}^t \},$$

$$(94)$$

with $\overline{\boldsymbol{U}}_{i,v,k,\mu,m,l,r,n}^{t}$ being given by

$$\operatorname{tr}\left\{\bar{\mathbf{g}}_{i,v,k,r,l}\mathbf{C}_{v,\mu,r}^{t-1,t-1}\widetilde{\mathbf{C}}_{i,m,l,n}^{t,t}\right\},\tag{95}$$

$$\mathbb{E}_{\mathbf{C}}\{|\mathrm{MLI}_{k,n,4,4}^{t}|^{2}\} \approx \sum_{\substack{i=1\\i\neq k}}^{K} \left(\sum_{l=1}^{L} \frac{|\widetilde{\mathbf{g}}_{i,k,l}^{(\mathrm{ef})}|^{4}}{n_{s}} + \sum_{l=1}^{L} \sum_{\substack{r=1\\r\neq l}}^{L} |\widetilde{\mathbf{g}}_{i,k,l}^{(\mathrm{ef})} \widetilde{\mathbf{g}}_{i,k,r}^{(\mathrm{ef})}|^{2} \left(\frac{1}{L_{k}} + \widetilde{L}_{k}\right)\right) + \sum_{\substack{i=1\\i\neq k}}^{K} \sum_{\substack{v=1\\v\neq k,v\neq i}}^{K} \sum_{l=1}^{L} \sum_{r=1}^{L} \frac{|\widetilde{\mathbf{g}}_{i,k,l}^{(\mathrm{ef})} \widetilde{\mathbf{g}}_{v,k,r}^{(\mathrm{ef})}|^{2}}{L_{k}}$$
(99)

where $\bar{\mathbf{g}}_{i,v,k,r,l} = (\tilde{\mathbf{g}}_{i,k,l}^{(\mathrm{ef})})^{\mathrm{H}} \tilde{\mathbf{g}}_{i,k,l}^{(\mathrm{ef})} (\tilde{\mathbf{g}}_{v,k,r}^{(\mathrm{ef})})^{\mathrm{H}} \tilde{\mathbf{g}}_{v,k,r}^{(\mathrm{ef})}$. Moreover, $\tilde{\mathbf{C}}_{i,m,l,n}^{t,t} = \mathbf{A}_n \big[\mathbf{C}_i^t \big]_{m(l,i),:}^{\mathrm{H}} \big[\mathbf{C}_i^t \big]_{m(l,i),:}^{\mathrm{H}} \mathbf{A}_n^{\mathrm{H}}$, and $\mathbf{C}_{v,\mu,r}^{t-1,t-1} = \big[\mathbf{C}_v^{t-1} \big]_{\mu(r,v),:}^{\mathrm{H}} \big[\mathbf{C}_v^{t-1} \big]_{\mu(r,v),:}^{\mathrm{H}}$. The term $\tilde{U}_{i,k,\mu,m,l,r,n}^t$ is obtained in (94) as

$$\operatorname{tr}\left\{\widetilde{\mathbf{g}}_{i,k,r,l}\mathbf{C}_{i,m,\mu,l,r}^{t-1,t-1}\widetilde{\mathbf{C}}_{i,\mu,m,r,l,n}^{t,t}\right\},\tag{96}$$

where we have $\widetilde{g}_{i,k,r,l} = (\widetilde{g}_{i,k,l}^{(ef)})^H \widetilde{g}_{i,k,l}^{(ef)} (\widetilde{g}_{i,k,r}^{(ef)})^H \widetilde{g}_{i,k,r}^{(ef)}$ and $\widetilde{\mathbf{C}}_{i,\mu,m,r,l,n}^{t,t} = \mathbf{A}_n [\mathbf{C}_i^t]_{\mu(r,i),:}^H [\mathbf{C}_i^t]_{m(l,i),:}^H \mathbf{A}_n^H$. Moreover, we have that $\mathbf{C}_{i,m,\mu,l,r}^{t-1,t-1} = [\mathbf{C}_i^{t-1}]_{m(l,i),:}^H [\mathbf{C}_i^{t-1}]_{\mu(r,i),:}^H$

To compute $\mathbb{E}_{\mathbf{C}}\{\overline{U}_{i,v,k,\mu,m,l,r,n}^t\}$ in (95) we have noted that $\mathbb{E}_{\mathbf{C}}\{\operatorname{tr}\{\mathbf{C}_{v,\mu,r}^{t-1,t-1}\widetilde{\mathbf{C}}_{i,m,l,n}^{t,t}\}\}$ is approximately

$$\mathbb{E}_{\mathbf{C}}\left\{\operatorname{tr}\left\{\mathbf{C}_{v,\mu,r}^{t-1,t-1}\widetilde{\mathbf{C}}_{i,m,l,n}^{t,t}\right\}\right\} \approx \begin{cases} 1/n_s & \text{if } \mu(r,v) = m(l,i).\\ 1/L_k & \text{otherwise,} \end{cases}$$

for v=i. In contrast, $\mathbb{E}_{\mathbf{C}}\left\{\operatorname{tr}\left\{\mathbf{C}_{i,m,\mu,l,r}^{t-1,t-1}\widetilde{\mathbf{C}}_{i,\mu,m,r,l,n}^{t,t}\right\}\right\}$ in (96) is calculated approximately as

$$\mathbb{E}_{\mathbf{C}}\left\{\operatorname{tr}\left\{\mathbf{C}_{i,m,\mu,l,r}^{t-1,t-1}\widetilde{\mathbf{C}}_{i,\mu,m,r,l,n}^{t,t}\right\}\right\} = \widetilde{L}_{k},\tag{98}$$

where $\widetilde{L}_k \approx 0$ for $L_k = 2$, $\widetilde{L}_k \approx 0.112$ for $L_k = 4$, and $\widetilde{L}_k \approx 1/L_k$ for $L_k = 8$. Finally, $\mathbb{E}_{\mathbf{C}}\{|\mathrm{MLI}_{k,n,4,4}^t|^2\}$ can be computed as in (99), which is shown at the top of the page.

REFERENCES

- M. M. M. Freitas, S. Buzzi, and G. Interdonato, "Eliminating phase misalignments in cell-free massive MIMO via differential transmission," *IEEE Wireless Commun. Lett.*, vol. 14, no. 9, pp. 2718–2722, Sep. 2025.
- [2] M. M. M. Freitas, S. Buzzi, and G. Interdonato, "UAV-empowered aerial cell-free networks robust to downlink phase misalignments," in Proc. IEEE Int. Workshop Signal Process. and AI for Wireless Commun. (SPAWC), Jul. 2025, pp. 1–5.
- [3] Ö. T. Demir, E. Björnson, and L. Sanguinetti, Foundations of User-Centric Cell-Free Massive MIMO. now publishers inc., 2021, vol. 14, no. 3-4. [Online]. Available: http://dx.doi.org/10.1561/2000000109
- [4] H. Q. Ngo, G. Interdonato, E. G. Larsson, G. Caire, and J. G. Andrews, "Ultradense cell-free massive MIMO for 6G: Technical overview and open questions," *Proc. of IEEE*, vol. 112, no. 7, pp. 805–831, Jul. 2024.
- [5] S. Buzzi, F. Linsalata, E. Moro, and G. Interdonato, "Why user-centric cell-free distributed MIMO systems will be the disruptive 6G technology," *TechRxiv*, Jul. 2025, submitted. [Online]. Available: http://dx.doi.org/10.36227/techrxiv.175355490.09511116/v1
- [6] R. Rogalin et al., "Scalable synchronization and reciprocity calibration for distributed multiuser MIMO," IEEE Trans. Wireless Commun., vol. 13, no. 4, pp. 1815–1831, Apr. 2014.
- [7] E. G. Larsson and J. Vieira, "Phase calibration of distributed antenna arrays," *IEEE Commun. Lett.*, vol. 27, no. 6, pp. 1619–1623, Jun. 2023.
- [8] Y. Cao et al., "Experimental performance evaluation of cell-free massive MIMO systems using COTS RRU with OTA reciprocity calibration and phase synchronization," *IEEE J. Sel. Areas Commun.*, vol. 41, no. 6, pp. 1620–1634, Jun. 2023.
- [9] S. Xu, Y. Cao, C. Li, D. Wang, and L. Yang, "Spanning tree method for over-the-air channel calibration in 6G cell-free massive MIMO," *IEEE Trans. Wireless Commun.*, vol. 22, no. 8, pp. 5567–5582, Aug. 2023.
- [10] E. G. Larsson, "Massive synchrony in distributed antenna systems," IEEE Trans. Signal Process., vol. 72, pp. 855–866, Jan. 2024.
- [11] S. Xu, Z. Zhang, Y. Xu, C. Li, and L. Yang, "Deep reciprocity calibration for TDD mmWave massive MIMO systems toward 6G," *IEEE Trans. Wireless Commun.*, vol. 23, no. 10, pp. 13285–13299, Oct. 2024.

- [12] U. Kunnath Ganesan, R. Sarvendranath, and E. G. Larsson, "BeamSync: Over-the-air synchronization for distributed massive MIMO systems," *IEEE Trans. Wireless Commun.*, vol. 23, no. 7, pp. 6824–6837, Jul. 2024.
- [13] K.-H. Ngo and E. G. Larsson, "Distributed MIMO with over-the-air phase calibration integrated into the TDD flow," 2025. [Online]. Available: https://arxiv.org/abs/2509.03722
- [14] H. Yan and I.-T. Lu, "Asynchronous reception effects on distributed massive MIMO-OFDM system," *IEEE Trans. Commun.*, vol. 67, no. 7, pp. 4782–4794, Jul. 2019.
- [15] J. Li, M. Liu, P. Zhu, D. Wang, and X. You, "Impacts of asynchronous reception on cell-free distributed massive MIMO systems," *IEEE Trans. Veh. Tech.*, vol. 70, no. 10, pp. 11106–11110, Oct. 2021.
- [16] Y. Fang, L. Qiu, X. Liang, and C. Ren, "Cell-free massive MIMO systems with oscillator phase noise: Performance analysis and power control," *IEEE Trans. Veh. Tech.*, vol. 70, no. 10, pp. 10048–10064, Oct. 2021.
- [17] Y. Qi, J. Dang, Z. Zhang, L. Wu, and Y. Wu, "Downlink precoding for cell-free FBMC/OQAM systems with asynchronous reception," *IEEE Commun. Lett.*, vol. 27, no. 9, pp. 2427–2431, Sep. 2023.
- [18] J. Zheng et al., "Asynchronous cell-free massive MIMO with rate-splitting," IEEE J. Sel. Areas Commun., vol. 41, no. 5, pp. 1366–1382, May 2023.
- [19] K. W. Helmersson, P. Frenger, and A. Helmersson, "Robust precoding weights for downlink D-MIMO in 6G communications," in *Proc. IEEE Globecom Workshops (GC Wkshps)*, Kuala Lumpur, Malaysia, Dec. 2023, pp. 1111–1116.
- [20] L. Qin et al., "A hybrid transmission scheme for cell-free massive MIMO systems with phase offset," in Proc. IEEE Veh. Tech. Conf. (VTC-Spring), Singapore, Jun. 2024, pp. 1–6.
- [21] U. Kunnath Ganesan, T. T. Vu, and E. G. Larsson, "Cell-free massive MIMO with multi-antenna users and phase misalignments: A novel partially coherent transmission framework," *IEEE Open J. Commun.* Soc., vol. 5, pp. 1639–1655, Mar. 2024.
- [22] R. P. Antonioli, I. M. Braga, G. Fodor, Y. C. Silva, and W. C. Freitas, "Mixed coherent and non-coherent transmission for multi-CPU cell-free systems," in *Proc. IEEE Int. Conf. Commun. (ICC)*, Rome, Italy, May 2023, pp. 1068–1073.
- [23] R. Pinto Antonioli et al., "On the energy efficiency of cell-free systems with limited fronthauls: Is coherent transmission always the best alternative?" *IEEE Trans. Wireless Commun.*, vol. 21, no. 10, pp. 8729–8743, Oct. 2022.
- [24] L. Miretti, G. Caire, and S. Stańczak, "Robust mmWave/sub-THz multiconnectivity using minimal coordination and coarse synchronization," *IEEE Trans. Wireless Commun.*, vol. 24, no. 1, pp. 293–308, Jan. 2025.
- [25] C. D'Andrea et al., "Coherent vs. non-coherent joint transmission in cell-free user-centric non-terrestrial wireless networks," in Proc. IEEE Int. Workshop Signal Process. Adv. Wireless Commun. (SPAWC), Lucca, Italy, Sep. 2024, pp. 636–640.
- [26] E. G. Larsson and P. Stoica, "Space-time block coding for wireless communications," Cambridge University Press, 2003.
- [27] M. M. M. Freitas et al., "Scalable user-centric distributed massive MIMO systems with restricted processing capacity," *IEEE Trans. Wireless Commun.*, vol. 23, no. 12, pp. 19 933–19 949, 2024.
- [28] E. Nayebi, A. Ashikhmin, T. L. Marzetta, H. Yang, and B. D. Rao, "Precoding and power optimization in cell-free massive MIMO systems," *IEEE Trans. Wireless Commun.*, vol. 16, no. 7, pp. 4445–4459, Jul. 2017.
- [29] G. Interdonato, P. Frenger, and E. G. Larsson, "Scalability aspects of cell-free massive MIMO," in *Proc. IEEE Int. Conf. Commun. (ICC)*, May 2019, pp. 1–6.
- [30] S. Chen, J. Zhang, E. Björnson, Ö. T. Demir, and B. Ai, "Energy-efficient cell-free massive MIMO through sparse large-scale fading processing," *IEEE Trans. Wireless Commun.*, vol. 22, no. 12, pp. 9374–9389, 2023.
- [31] 3GPP, Study on channel model for frequencies from 0.5 to 100 GHz, 2019, 3GPP TR 38.901 (Release 16).
- [32] 3GPP, NR; User Equipment (UE) radio transmission and reception; Part 1: Range 1 Standalone, 2021, 3GPP TR 38.101-1 (Release 17).